NASA/CR-2006-214520

Configuration and Sizing of a Test Fixture for Panels Under Combined Loads

Andrew E. Lovejoy
Analytical Services & Materials, Inc., Hampton, Virginia

October 2006

The NASA STI Program Office . . . in Profile

Since its founding, NASA has been dedicated to the advancement of aeronautics and space science. The NASA Scientific and Technical Information (STI) Program Office plays a key part in helping NASA maintain this important role.

The NASA STI Program Office is operated by Langley Research Center, the lead center for NASA's scientific and technical information. The NASA STI Program Office provides access to the NASA STI Database, the largest collection of aeronautical and space science STI in the world. The Program Office is also NASA's institutional mechanism for disseminating the results of its research and development activities. These results are published by NASA in the NASA STI Report Series, which includes the following report types:

- TECHNICAL PUBLICATION. Reports of completed research or a major significant phase of research that present the results of NASA programs and include extensive data or theoretical analysis. Includes compilations of significant scientific and technical data and information deemed to be of continuing reference value. NASA counterpart of peer-reviewed formal professional papers, but having less stringent limitations on manuscript length and extent of graphic presentations.

- TECHNICAL MEMORANDUM. Scientific and technical findings that are preliminary or of specialized interest, e.g., quick release reports, working papers, and bibliographies that contain minimal annotation. Does not contain extensive analysis.

- CONTRACTOR REPORT. Scientific and technical findings by NASA-sponsored contractors and grantees.

- CONFERENCE PUBLICATION. Collected papers from scientific and technical conferences, symposia, seminars, or other meetings sponsored or co-sponsored by NASA.

- SPECIAL PUBLICATION. Scientific, technical, or historical information from NASA programs, projects, and missions, often concerned with subjects having substantial public interest.

- TECHNICAL TRANSLATION. English-language translations of foreign scientific and technical material pertinent to NASA's mission.

Specialized services that complement the STI Program Office's diverse offerings include creating custom thesauri, building customized databases, organizing and publishing research results ... even providing videos.

For more information about the NASA STI Program Office, see the following:

- Access the NASA STI Program Home Page at ***http://www.sti.nasa.gov***

- E-mail your question via the Internet to help@sti.nasa.gov

- Fax your question to the NASA STI Help Desk at (301) 621-0134

- Phone the NASA STI Help Desk at (301) 621-0390

- Write to:
  NASA STI Help Desk
  NASA Center for AeroSpace Information
  7121 Standard Drive
  Hanover, MD 21076-1320

NASA/CR-2006-214520

Configuration and Sizing of a Test Fixture for Panels Under Combined Loads

Andrew E. Lovejoy
Analytical Services & Materials, Inc., Hampton, Virginia

National Aeronautics and
Space Administration

Langley Research Center
Hampton, Virginia 23681-2199

Prepared for Langley Research Center
under Contract NNNL04AA10B

October 2006

Available from:

NASA Center for AeroSpace Information (CASI)
7121 Standard Drive
Hanover, MD 21076-1320
(301) 621-0390

National Technical Information Service (NTIS)
5285 Port Royal Road
Springfield, VA 22161-2171
(703) 605-6000

Table of Contents

List of Figures

List of Tables

Abstract

Future air and space structures are expected to utilize composite panels that are subjected to combined mechanical loads, such as bi-axial compression/tension, shear and pressure. Therefore, the ability to accurately predict the buckling and strength failures of such panels is important. While computational analysis can provide tremendous insight into panel response, experimental results are necessary to verify predicted performances of these panels to judge the accuracy of computational methods. However, application of combined loads is an extremely difficult task due to the complex test fixtures and set-up required. Presented herein is a comparison of several test set-ups capable of testing panels under combined loads. Configurations compared include a D-box, a segmented cylinder and a single panel set-up. The study primarily focuses on the preliminary sizing of a single panel test configuration capable of testing flat panels under combined in-plane mechanical loads. This single panel set-up appears to be best suited to the testing of both strength critical and buckling critical panels. Required actuator loads and strokes are provided for various square, flat panels.

Introduction

Future air and space structures, such as the blended wing body aircraft shown in Figure 1, are expected to utilize composite panels that are subjected to combined mechanical loads. Combined loads can include internal pressure and in-plane mechanical loads, such as bi-axial compression/tension, including in-plane bending, and shear. Therefore, the ability to accurately predict the buckling and strength failures of panels under such loading is important. While computational analysis can provide tremendous insight into the panel response, experimental results are necessary to verify predicted performances of these panels to judge the accuracy of computational methods. However, application of combined loads is an extremely difficult task due to the complex test fixtures and set-up required. Few examples of test set-ups capable of applying these combined loads have been found in the literature.

Musgrove and Green [1] conducted tests on 40-inch, square panels in a combined-load fixture. The panel was clamped on one edge. Axial compression and shear loads were applied to edge opposite the clamped edge. The remaining two edges were free. Out-of-plane bending loads could be applied using an airbag system.

Percy [2] examined square, flat panels having hat stiffeners that were tested and analyzed under combined mechanical and thermal loads. Mechanical loads included axial compression and end shear. Panels were made from titanium or titanium matrix composite.

Martin and McWithey [3] described a test apparatus for the combined loading of flat panels that consisted of a disk-shaped fixture, within which was embedded a square or rectangular test section. Loads were to be applied through a series of rods attached to the test fixture edge, and it is the orientation of these load rods with respect to the test section that provides the combined load state. The theoretical test apparatus described would permit running loads of up to 10kips/in on a 48-inch-diameter fixture, with a 24-inch square test section. Computational analysis was used to examine the effectiveness of the test apparatus, but no actual test facility was produced or used.

Romeo and Frulla [4-7] and Romeo [8] developed and utilized a test apparatus capable of applying combined loads to study panels for sizes up to 700 mm by 1000 mm (27.56 in. by 39.37 in.). Longitudinal load was applied by two separately-controlled servo-actuators, and displacement control was used to maintain panel ends remaining parallel. Transverse load was also applied by two separately-controlled servo-actuators with displacement control used to maintain panel ends parallel. Shear load was applied to the bottom end of the panel by one servo-actuator. The test fixture is composed of load and support frames constructed from steel and aluminum, with the load frames being L-shaped steel rails bolted to the four edges of the specimen. This set-up appears to be the most comprehensive and versatile found in the literature.

Featherston and Ruiz [9, 10] developed and used a test set-up capable of applying a shear load at the specimen end that is opposite a clamped end, the other two opposite edges being simply-supported. By keeping the end to which the load is applied parallel to the clamped end, in-plane bending is created in addition to the shear. However, the specimens are small (< 200 mm (7.87 in.) on an edge), curved panels representative of turbine blades and biaxial loads are not possible.

A test machine capable of applying axial load or bending, shear and torsion, and internal pressure to a D-box fixture was described by Ambur, Cerro and Dickson [11]. Several researchers, including Rouse, Young and Gehrki [12], used the NASA Langley Research Center (LaRC) D-box to study a stiffened aluminum curved panel. Curved panels subjected to combined mechanical load and internal pressure have been simulated using the D-box test fixture. In practice, however, this apparatus appears to be practical for applying uniaxial load and shear load even though it has internal actuators that are used to provide hoop loads. A biaxial stress state is achieved using internal pressure, but end effects restrict the effective test section to the center of the panel. Test panels typically tested the D-box were 96 in. by 120 in. in size.

Lastly, Fields, Richards and DeAngelis [13] developed a combined loads fixture that was capable of testing 4-ft by 4-ft panels with combined axial (tension or compression) and shear loads at temperatures ranging from room temperature to 915 degrees F. Maximum axial loads were 3.4 kips/in. and 4.26 kips/in. in compression and tension, respectively. Maximum shear load was 1.06 kips/in. in the panel. However, again, biaxial loading was not possible.

Therefore, because few attempts have been made to experimentally examine the response of panels subjected to combined in-plane loads, a test set-up with fixtures capable of applying combined biaxial, in-plane bending and shear loads is needed to understand the behavior of components that are expected in future air and space vehicles. The set-up should be capable of being modified to incorporate pressure load, as well.

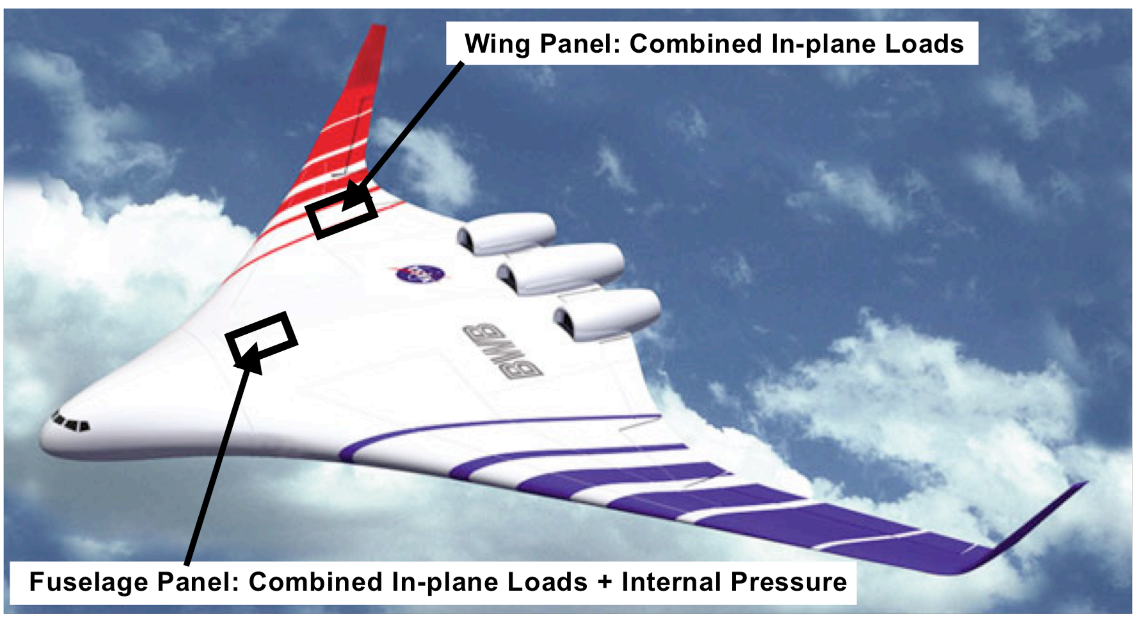

Figure 1: Conceptual design of a BWB aircraft

Requirements

In general, the panels associated with future air and space structures can have complex curvature and any stacking sequence. These panels will be subjected to combined loads including pressure. Accurate testing of such panels requires a set-up capable of applying combined loads and pressure simultaneously, while maintaining realistic boundary conditions. The test fixture and set-up should provide the capability of:

1) Mounting test specimens ranging from smaller size strength specimens (up to 10 in. square (see Figure 2)) to larger buckling specimens (3 ft. by 4 ft. or larger (see Figure 3)).

2) Handling specimens of greatly varying curvatures (radii of curvature ranging from 10 in. to 180 in. or more).

3) Applying bi-axial compression/tension and shear.

4) Applying pressure on one surface of the panel.

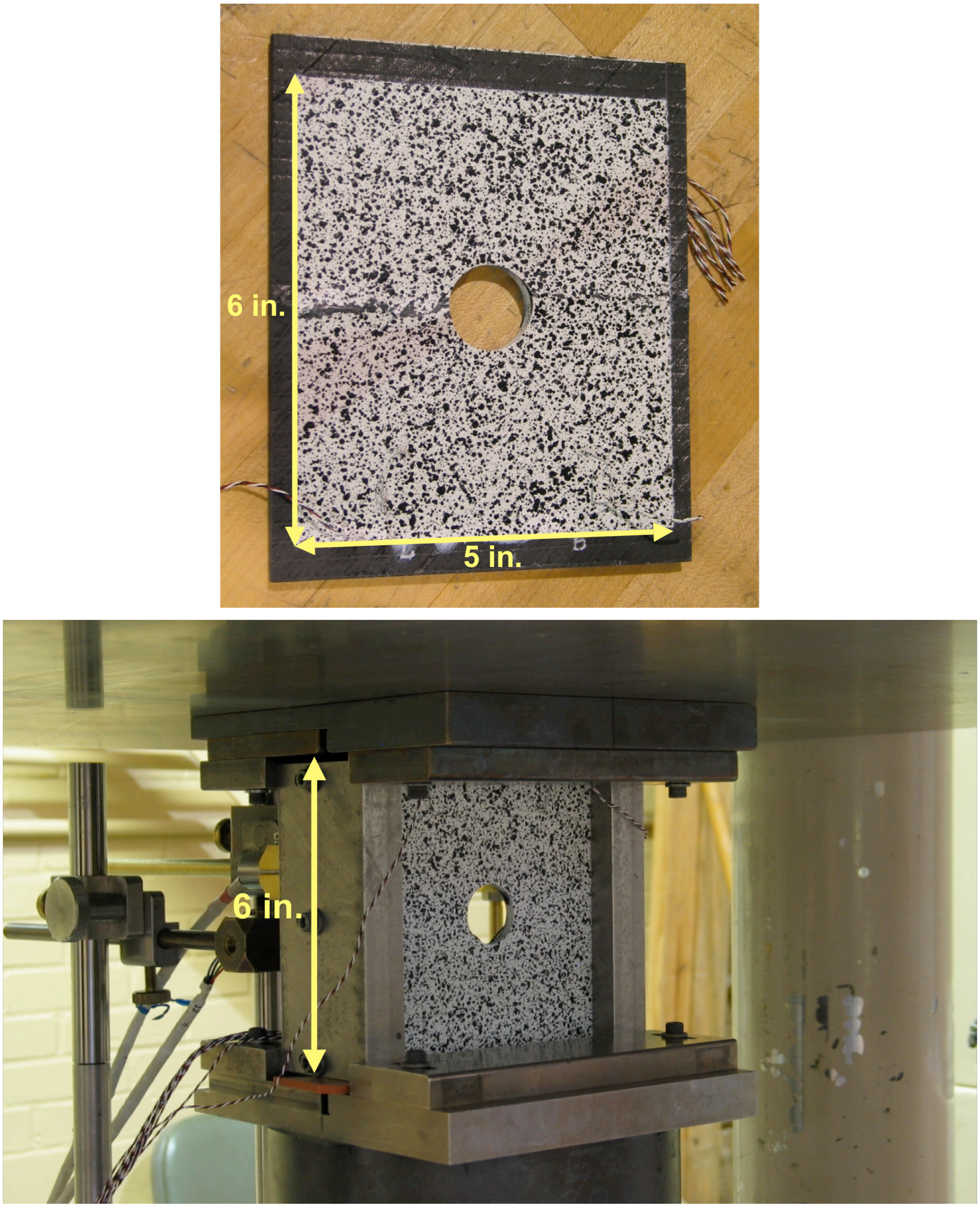

Figure 2: Typical 5-in. by 6-in. strength test specimen (with hole) and test set-up

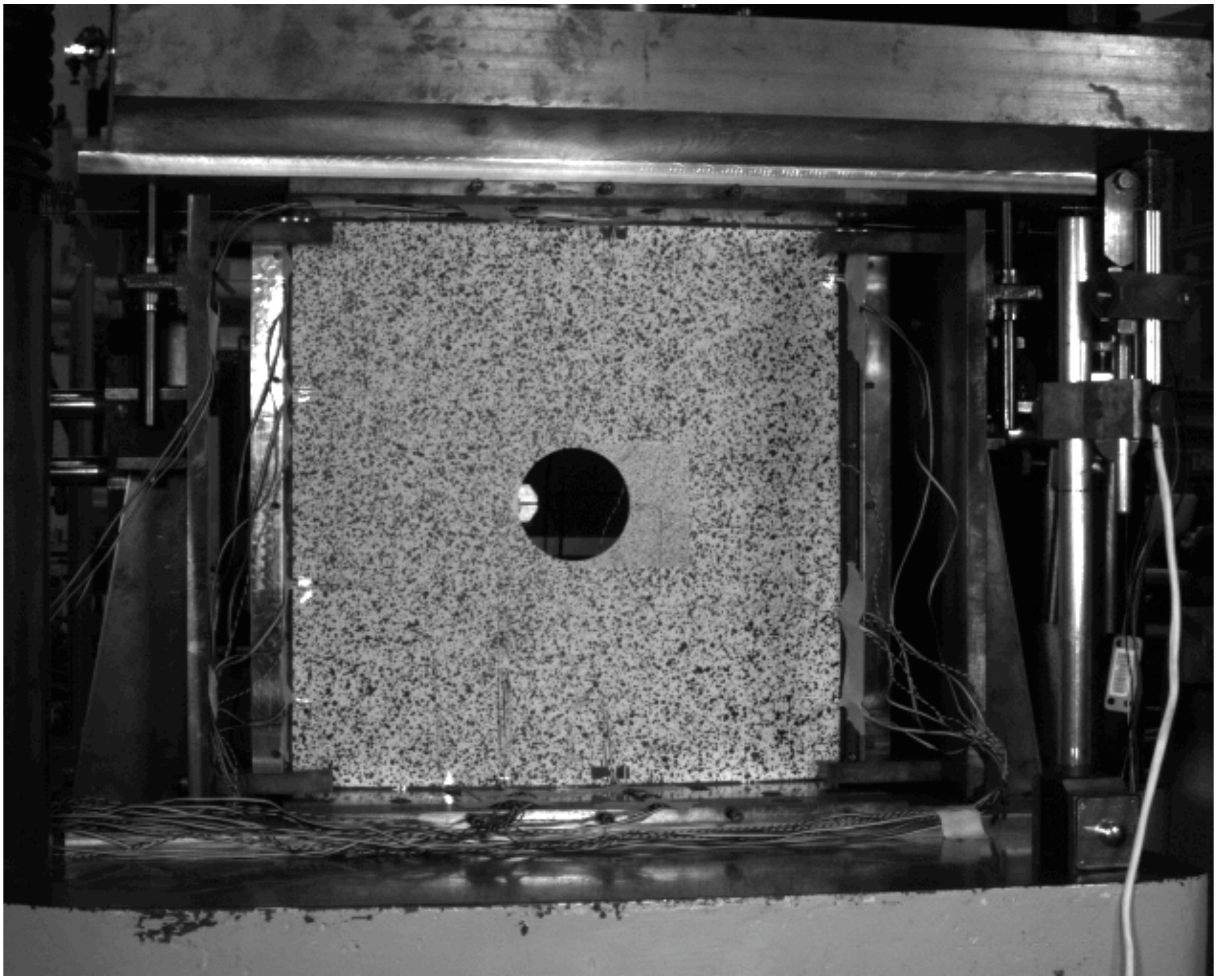

Figure 3: Typical 14-in. by 14-in. buckling test specimen (with hole) and test set-up

Test Configuration Options

In order to satisfy the combined-load test set-up requirements, several test configuration options were considered. The test configuration options considered include a D-box, a segmented cylinder, and an individual panel. Each of these configurations offers it's own advantages and limitations that are discussed in the following sections. Discussions and results are provided for the D-box and segmented cylinders configurations. Discussion and results are then given for the preliminary sizing of a test configuration for an individual panel set-up.

D-Box

A D-box is a fixture on which a test panel can be mounted that when viewed in cross-section has a "D" shape. Such a fixture has been used for large panels that can be tested in the COmbined Loads Test System (COLTS) facility [11, 13]. Figure 4 shows the COLTS facility, where the large cylindrical test specimen is in the place where the D-box fixture and a test panel are mounted. For the D-box shown in the figure, tests panels are approximately 96 in. by 120 in., and have a 125 in. radius of curvature. The benefits and disadvantages of such a test configuration are summarized in Table 1. The major advantages are the ability to easily pressurize the panel and to test panels of various curvatures. The facility shown is

Figure 4 is geared towards large-scale panels only and will not satisfy the requirement for testing smaller strength-critical panels.

Another test facility presently at LaRC is the bending, shear and torsion test facility, herein designated the Combined Loads Apparatus (CLA) facility, and shown in Figure 5. CLA is capable of handling complete cylinders with a maximum radius of 18 inches. A D-box fixture was considered for use in the CLA facility. Figure 6 shows a sketch of the D-box cross-section and the related geometric parameters. A simple example of a test panel in pure shear, equivalent to a full cylinder in torsion, demonstrates that the CLA is incapable of correctly utilizing a D-box test fixture in it's current configuration. The kinematics of the pure shear example are shown in Figure 7. The figure shows the original position of the panel (red) and D-box fixture (blue), and successive positions of the panel and D-box if the panel were part of a full cylinder rotated about its axis 15, 30 and 45 degrees. For the CLA and D-box configuration to produce the same position for the panel, the D-box must undergo a rotation and axis translation. The vectors in the figure show the translation vectors required for the 15-, 30- and 45-degree rotations, respectively. These translation vectors are a function of the geometric parameters, including the offset between the center of the full cylinder and the D-box, and require that the end platen be able to rotate and to translate in two dimensions. However, the CLA facility has only three actuators, all of which are oriented in the same direction. Therefore, the CLA end platen is capable of rotation, but is only capable of translation in a single direction. For small amounts of rotation the resulting error is small, but as the applied rotation increases, the error associated with the incorrect translation direction increases. The CLA facility is not capable of utilizing the D-box concept with the current actuator arrangement. However, it may be possible to adjust the actuator arrangement to facilitate the use of a D-box in CLA.

Table 1: Features, benefits and disadvantages of a D-box test configuration

Features	Benefits	Disadvantages
• "Accordion" construction. • Constructed from repeated I-beam segments. • D-box replaces significant portion of a complete cylinder.	• Fabrication from repeated I-beam segments permits variable D-box (hence panel) lengths. • Low axial stiffness puts load into test panel. • Can accommodate panels of varied radii. • Eliminates the need to construct complete cylinders. • Easily pressurized.	• Can not get biaxial tension/ compression without internal actuators. • Practical test region is at center of panel due to end effects where attached to platens. • Not readily applicable to smaller, strength-critical specimens. • Best suited to cylindrical panels and not doubly-curved panels.

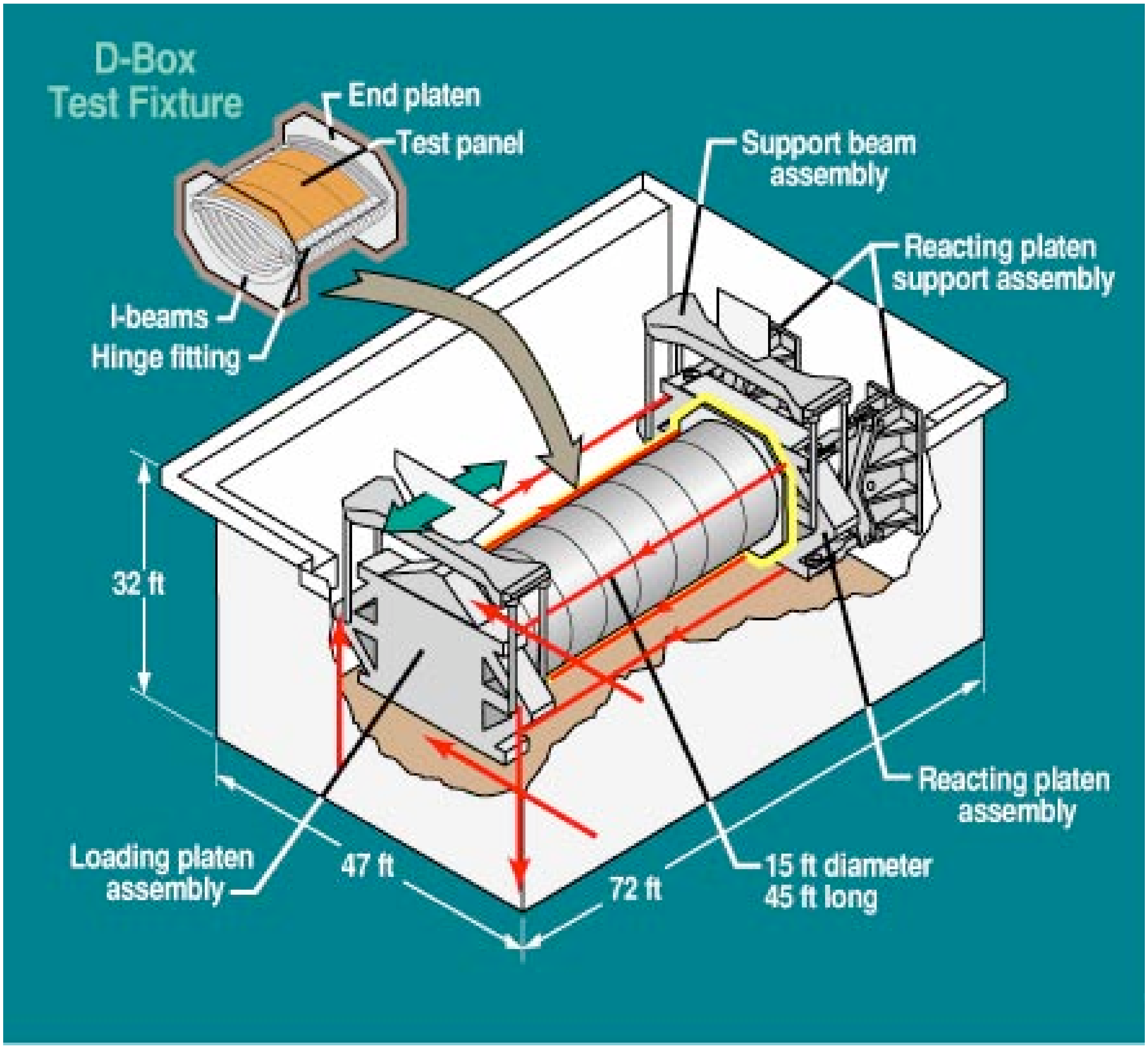

Figure 4: NASA LaRC COLTS D-box replaces fuselage section in COLTS facility

Figure 5: NASA LaRC bending, shear and torsion facility (CLA) with cylindrical test specimen

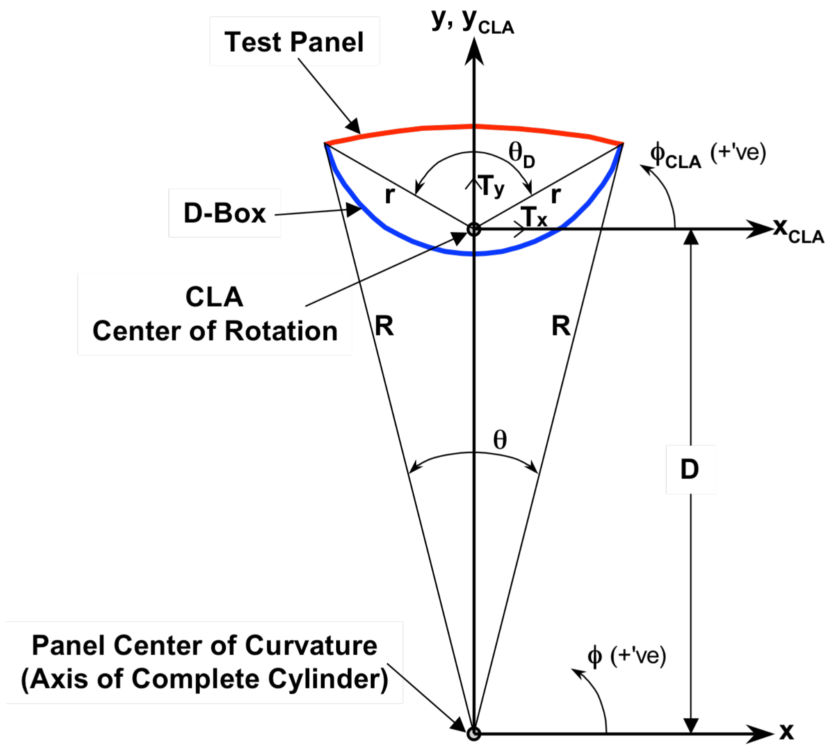

(+'ve) indicates positive direction

Figure 6: CLA D-box and panel configuration with parameter definitions

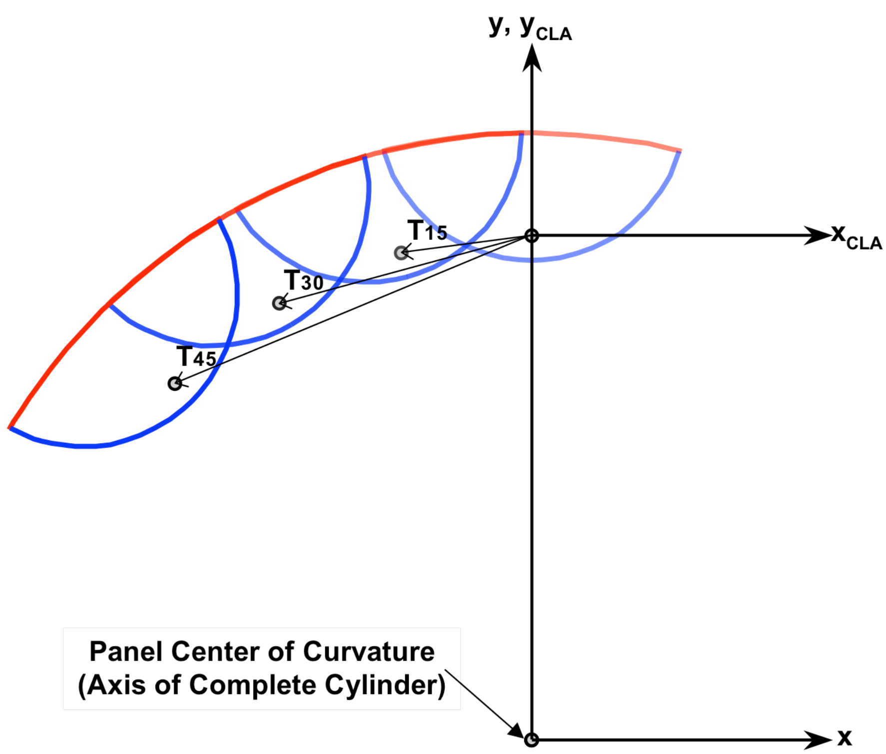

Figure 7: Kinematics of D-box configuration for cylinder torsion

Segmented Cylinder

A second concept considered was that of a segmented cylinder. This concept was used by Wilkins and Olson [14] to examine shear buckling of composite curved panels. A segmented cylinder consists of several cylindrical panels that are attached together to make a complete cylinder. Fittings at the ends of the cylinder attach it to the test apparatus, such as the CLA facility shown in Figure 5. A generic illustration of the segmented cylinder concept is shown in Figure 8. The features, benefits and disadvantages of such an approach are given in Table 2.

A study was undertaken to design a segmented, cylindrical fixture for testing panels in the CLA facility. Actuators for the CLA facility are currently capable of a maximum load of 50 kips. However, it was decided that the actuator load at panel buckling should not exceed 80% of the actuator limit, and therefore the maximum allowable actuator load for the study was limited to 40 kips. The initial design considered only torsional loading. Compression was to be studied later depending upon the results of the torsion study. For the current study, the test panel was assumed to have a radius of 18 in. (the maximum possible in the CLA), a height of 18 in., an arc length of 18 in., and thicknesses ranging from 0.04 to 0.12 inches. Test panels used in this study were made from aluminum. The segmented cylinder fixture consists of 5 parts that are connected to each other and to the panel via stiffener flanges. Five segments were chosen so that each of the segments would be similar in size to the test panel in an attempt to minimize the likelihood of segment buckling. There were three types of segmented cylinder construction considered in this study; monocoque, stiffened and sandwich. The CLA facility itself is constructed from steel. The finite element mesh and the location of the test panel within the mesh are shown in Figure 9.

The monocoque construction was examined first and was given an initial segment thickness of 0.1 in. for all sections. Segment thickness was increased for larger thickness test panels. Segments of the segmented cylinder fixture were assumed to be made of steel. Table 3 shows the actuator loads required for panel buckling using the monocoque segmented cylinder fixture for various segment and panel thicknesses. The values reported used a more coarse mesh than that shown above, so the force values will decrease with the refined mesh. It can be seen that the maximum realistic segment thickness is 0.1 in. and that the maximum panel thickness that can be tested is slightly less than 0.08 in. for the current CLA configuration and actuators.

The next design possibility for the segmented cylinder fixture involves a less-thick shell that is grid stiffened. The reduced segment thickness results in lower actuator forces, and the stiffeners are used to prevent buckling of the segments. Stiffener patterns used in the study are shown in Figure 10. Note that the stiffeners do not extend to the edges of the segment. Also, the thickness of the segment between the stiffeners ends and the segment edges was set to be 0.1 in. thick, while the main body of the segment where the stiffeners are located was varied in thickness. Table 4 shows the actuator loads for panel buckling for the stiffened segmented cylinder for various thicknesses of segments and panels and stiffener pattern. The thickest panel that can be tested using the configurations studied is the 0.08 in. thickness panel with stiffener pattern three and 0.05 in. thick segments. However, note that using the grid-stiffened segments, it is possible to lower the actuator force required to buckle a 0.12 in. thick panel when compared to a complete cylinder, with actuator forces of approximately 66 kips and 70 kips, respectively. It is anticipated that additional stiffener patterns may result in even lower actuator forces, but a 0.1 in. thick test panel will probably be the thickest panel that can be tested with the current CLA actuators.

A segmented cylinder fixture of sandwich construction was the last design examined. The faces of the sandwich segments were aluminum, and the core was specified as a material with essentially no extensional stiffness and a shear modulus of either 1000 ksi or 10 ksi. Face and core thicknesses were varied to study the effect of sandwich geometry on the actuator forces. Table 5 lists the panels studied and the required actuator forces. From the results shown in the table, it is clearly seen that the core material should have the lower value for the shear modulus. Also, to obtain thicker test specimens, the core thickness should be increased and the skin thickness decreased. Using the sandwich segments with skin thickness of 0.02 in. and core thickness of 0.4 in., 0.1 in. is the maximum panel thickness that can be tested with the current CLA configuration and actuators. Of the segmented cylinder fixture constructions examined, the sandwich construction can handle the thickest test panel, as shown in Table 6.

Table 2: Features, benefits and disadvantages of the segmented cylinder test fixture

Features	Benefits	Disadvantages
• Constructed from replaceable segments. • Segmented cylinder replaces significant portion of a complete cylinder.	• Test panels easily swapped in and out for testing. • Eliminates the need to construct complete cylindrical panels. • Easily pressurized	• Can not get biaxial tension/ compression. • Best suited to cylindrical panels and not double-curved panels. • Stiffeners connecting segments and panel significantly increase overall axial stiffness.

Table 3: Actuator forces for monocoque segmented cylinder under pure torsion

Panel Thickness (in.)	Segment Thickness (in.)	Actuator Force (lbs.)
0.04	0.1	13,386
0.06	0.1	25,513
0.08	0.1	41,296
0.1	0.1	60,284*
0.12	0.1	85,749**
0.12	0.12	85,063***
0.12	0.13	97,681
0.12	0.15	104,760
0.12	0.2	120,950

* Buckling not in panel but in segmented cylinder.
** Segments bisected vertically by additional stiffeners to prevent segment buckling.
*** Used refined model above and buckling not in panel. Note that a full 0.12 unstiffened cylinder results in an actuator force of 69,956 lbs. at buckling.

Table 4: Actuator forces for stiffened segmented cylinder under pure torsion

Stiffener Pattern	Panel Thickness (in.)	Segment Thickness (in.)	Actuator Force (lbs.)
1	0.12	0.05	19867*
1	0.12	0.08	59686*
2	0.12	0.05	30085*
2	0.08	0.06	30076
2	0.1	0.06	46886
2	0.12	0.06	47745*
3	0.08	0.05	27859
3	0.08	0.06	30283
3	0.08	0.07	32513
3	0.08	0.08	34582
3	0.1	0.05	42772**
3	0.1	0.06	45895
3	0.1	0.07	49078
3	0.1	0.08	52026
3	0.12	0.05	45410*
3	0.12	0.06	65685
3	0.12	0.07	69704
3	0.12	0.08	73693

* Buckling not in panel but in segmented cylinder.
** Buckling primarily in panel, but significant buckling in segmented cylinder.

Table 5: Actuator forces for sandwich segmented cylinder under pure torsion

Core Shear Modulus (ksi)	Panel Thickness (in.)	Segment Thicknesses (in.) (skin/core/skin)	Actuator Force (lbs.)
1000	0.04	0.04 / 0.2 / 0.04	15590
10	0.04	0.04 / 0.2 / 0.04	11740
10	0.04	0.03125 / 0.2 / 0.03125	10104
1000	0.06	0.04 / 0.2 / 0.04	29464
10	0.06	0.04 / 0.2 / 0.04	22602
10	0.06	0.03125 / 0.2 / 0.03125	19711
1000	0.08	0.04 / 0.2 / 0.04	47520
10	0.08	0.04 / 0.2 / 0.04	36931
10	0.08	0.03125 / 0.2 / 0.03125	32482
10	0.08	0.02 / 0.3 / 0.02	26157
10	0.08	0.02 / 0.4 / 0.02	24038*
1000	0.1	0.04 / 0.2 / 0.04	70001
10	0.1	0.04 / 0.2 / 0.04	55012
10	0.1	0.03125 / 0.2 / 0.03125	48755
10	0.1	0.02 / 0.3 / 0.02	39812
10	0.1	0.02 / 0.4 / 0.02	37001*
10	0.12	0.025 / 0.3 / 0.025	62675
10	0.12	0.02 / 0.3 / 0.02	57003
10	0.12	0.02 / 0.4 / 0.02	53383*

* Indicates results for model shown in Figure 9, all other results for coarse model having one forth the mesh density.

Table 6: Maximum panel thicknesses and actuator loads for the segmented-cylinder test constructions

Segmented Cylinder Construction	Maximum Panel Thickness (in.)	Maximum Actuator Load (kips)
Monocoque	0.08	41
Grid Stiffened	0.08	28
Sandwich	0.1	37

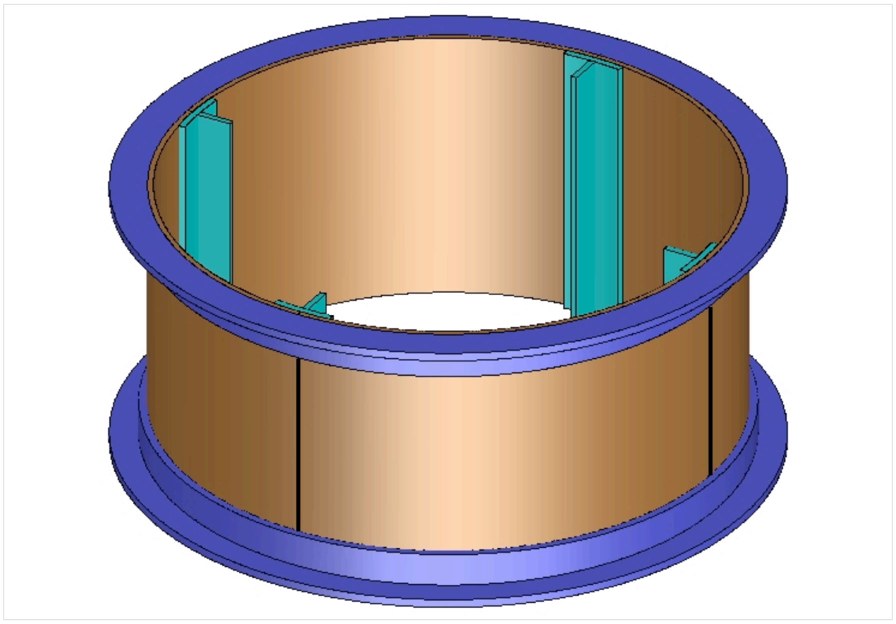

Figure 8: Generic, 4-section, segmented-cylinder test fixture illustration

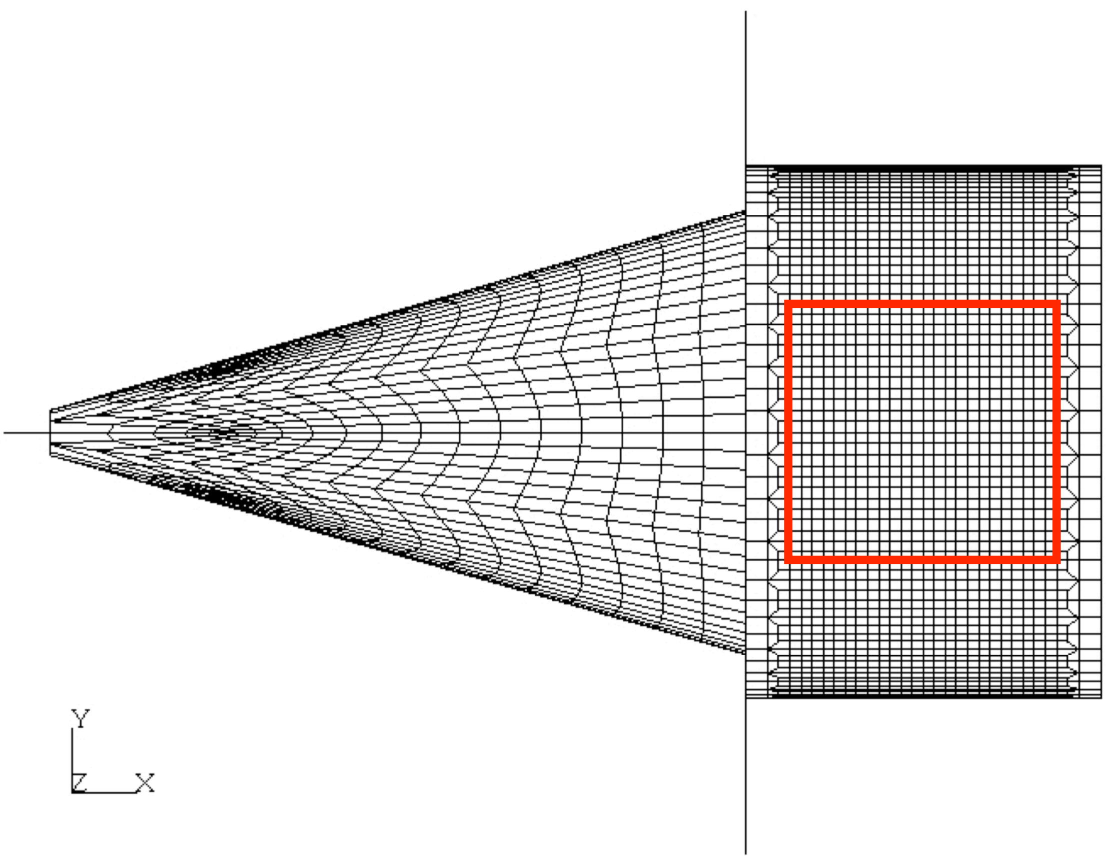

Figure 9: CLA and segmented-cylinder test fixture finite element mesh (test panel outlined in red)

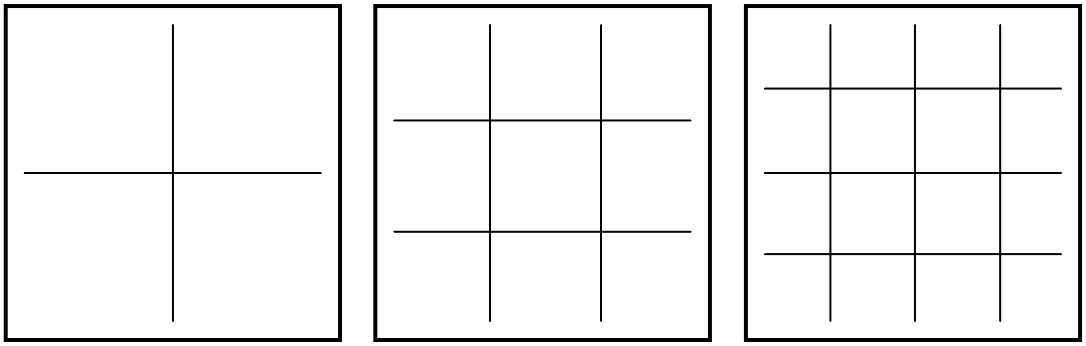

Figure 10: Stiffener patterns considered for stiffened segmented cylinder fixture

Single Panel

A single-panel test configuration consists of actuators and fixtures in which a single panel is mounted. Such an approach was utilized by Romeo and Frulla [4-7] and Romeo [8] for panels up to 27.56 in. by 39.37 in. (700 mm by 1000 mm). The test apparatus and set-up used in the references is shown in Figure 11. As mentioned earlier, this set-up seems to be the most comprehensive and versatile found in the literature. Table 7 lists the features, benefits and disadvantages of the single-panel test configuration. This test set-up essentially utilizes a picture frame configuration to transfer the loads into the test section. Picture frame fixtures have been used quite often in the past to test panels, and have even been used for curved panels. For example, Wolf and Kossira [15] used the picture frame method to study the shear response of curved panels. However, it is noted that the picture frame concept does not apply the shear along the curved edge (i.e., the shear is not tangent to the panel along the curved edge), but rather applies shear parallel to the chord of the curved edge, which can introduce significant eccentricity as the panel becomes less shallow. Therefore, due to the complexity of the test configuration needed to produce combined loads, especially on curved edges, it was decided to first focus on flat, square panels. The current study involves the development of a test set-up that can be used to test flat panels under combined loads. Figure 12 shows two such configurations, where the details of the fixtures and surrounding infrastructure are ignored until the detailed design phase. In the figure, the first sketch in parts a) and b) shows the actuator locations and the second sketch shows the direction of the actuator forces. The apparatus considered has two actuators for each of the biaxial loads, and one actuator for the shear load. This is set-up is similar in nature to that of Romeo and Frulla [4-7] and Romeo [8]. In order to provide preliminary load information for sizing of the test fixture and load cells, an analytical study was carried out for square panels of various areas, thicknesses and loads. Analyses were completed, and information needed for sizing of the test apparatus was compiled. The panels studied in this investigation are presented in Table 8.

Analyses were carried out using panel models generated in PATRAN [16] and analyzed using STAGS [17]. Only the panels were modeled, and it was assumed that the proposed set-up would result in the loading shown in Figure 13. The boundaries of the panel were assumed to be clamped for all analyses. The clamped boundary conditions applied, shown in Figure 13, were on the transverse (z) displacement, w, and on the rotations about the x-, y- and z-axes, denoted by θ_x, θ_y and θ_z, respectively. Rigid body motion was restrained by setting the x-displacement along the x = 0 edge equal to zero, and by restraining the y-displacement to zero at the panel coordinate system origin as shown in the figure. The load conditions, summarized in Table 9, all have a tension component, with either uniform compression, linearly varying compression or shear added. STAGS will permit uniform element edge loads, but not linearly varying edge loads. Therefore, variable edge loads must be applied as calculated nodal loads. In order to maintain uniformity in all analyses, all loads were applied as calculated nodal loads.

Finite element analyses were carried out to determine the buckling and strength response of the panels. Linear bifurcation analyses were used to determine the buckling load factors, and linear static analyses were used to determine the stress/strain state. Material failure was calculated using the computed stress state and the Tsai-Hill failure theory. The panels studied are assumed to be in plane stress with the failure index is defined as:

$$FI = \frac{\sigma_1^2}{X^2} - \frac{\sigma_1 \sigma_2}{X^2} + \frac{\sigma_2^2}{Y^2} + \frac{\tau_{12}^2}{S^2}$$

The values X, Y, and S in the equation are the lamina strengths. When the failure index exceeded unity, then the panel was deemed to have failed. For lamina that are oriented at an angle θ, the stresses must be transformed by the familiar transformation,

$$\begin{Bmatrix} \sigma_1 \\ \sigma_2 \\ \tau_{12} \end{Bmatrix} = \begin{bmatrix} \cos^2\theta & \sin^2\theta & 2\sin\theta\cos\theta \\ \sin^2\theta & \cos^2\theta & -2\sin\theta\cos\theta \\ -\sin\theta\cos\theta & \sin\theta\cos\sigma & \cos^2\theta - \sin^2\theta \end{bmatrix} \begin{Bmatrix} \sigma_x \\ \sigma_y \\ \tau_{xy} \end{Bmatrix}$$

A Tsai-Hill failure index was calculated for each ply orientation (45, -45, 0, and 90 degrees), and the maximum value assigned to the panel for determination of failure.

Table 10 shows the analysis matrix that was used to conduct the study. It includes load cases, dimensions and stacking sequences for the analyses conducted. The resultant actuator loads presented in this report are for each actuator. Thus, the total tension or compression load is divided into two actuators, and the shear load is applied by the single shear actuator. For the linearly varying loads, the actuator forces represent the in-plane bending couple force required to create the equal and opposite linear distribution, or is the differential force needed to create the linear distribution that becomes zero at one end.

Tables 11 – 21 show the actuator forces for the buckling analysis panels, and Tables 22 – 32 show the corresponding actuator strokes. In the tables, (+/-) indicates that the force/displacement is applied at both actuators but they are equal and opposite, while (+/0) indicates that the force/displacement is applied at one actuator and at the other actuator the force/displacement is zero. Also, for the values supplied in the tables, it was assumed that the actuators are aligned with the edges of the panel and reflect the configuration shown in Figure 13, part b).

Figures 14 – 24 show the mode shapes for the flat, square panels studied via buckling analysis. Since changing the direction of the shear has no effect on the strength determined failure load, the load cases were limited to the four shown in Table 10. Tables 33 – 36 show the actuator loads for the strength analysis panels, and Tables 37 – 40 show the corresponding actuator strokes.

The raw data can be plotted in several ways to visualize the responses of the panels. Figures 25 – 30 show actuator forces for several strength and buckling cases. Figures 31 – 36 show actuator forces as a function of strain for several buckling cases. Examination of the raw data and plots such as those presented will permit the sizing of panels that can be tested for various actuator set-ups. In the figures shown, it is assumed that the actuators are limited to 60 kips and the maximum strain is limited to 0.01. Therefore, the lower left portion of the plots represents the panels that could be tested using this set-up.

Table 7: Features, benefits and disadvantages of single panel test configuration

Feature	Benefit	Disadvantage
• Two pairs of biaxial actuators and a single shear actuator. • Single panel required to fit into apparatus.	• Test panels easily swapped in and out for testing. • Easily applies biaxial tension/ compression and shear.	• Not easily pressurized without additional fixturing • For practical purposes, limited to flat panels. • Require fixtures for each size test panel.

Table 8: Preliminary test fixture sizing panel definitions

Dimension (square)	Stacking Sequences*	Analyses
5 in.	$[45/-45/0/90]_{ns}$ n = 1,2,3,4,5,6,7	Strength, Buckling
8 in.	$[45/-45/0/90]_{ns}$ n = 1,2,3,4,5,6,7	Strength
10 in.	$[45/-45/0/90]_{ns}$ n = 1,2,3,4,5,6,7	Strength
14 in.	$[45/-45/0/90]_{ns}$ n = 1,2,3,4,5,6,7	Strength, Buckling
21 in.	$[45/-45/0/90]_{ns}$ n = 1,2,3,4,5,6	Buckling
28 in.	$[45/-45/0/90]_{ns}$ n = 1,2,3,4,5,6	Buckling

* n = 7 used for strength analyses only.

Table 9: Load case definitions

Load Condition Type	Ratio	Designation	Representation
Tension/Compression	$N_{y,max}/N_{x,max} = 1.0$	TC	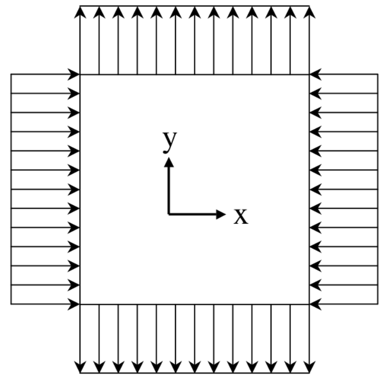
Tension/Shear	$N_{y,max}/N_{xy,max} = 2.0$	TS_2	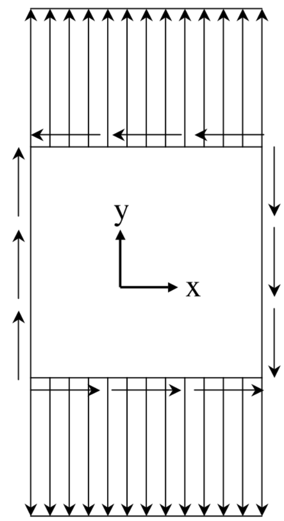
Tension/Shear	$N_{y,max}/N_{xy,max} = 1.0$	TS_1	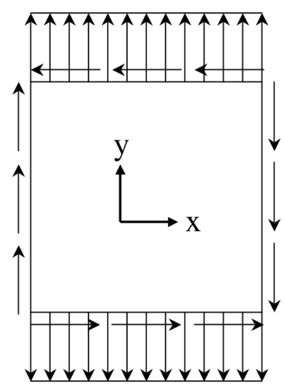

Table 9 (cont.): Load case definitions

Load Condition Type	Ratio	Designation	Representation
Tension/Shear	$N_{y,max}/N_{xy,max} = 0.5$	TS_05	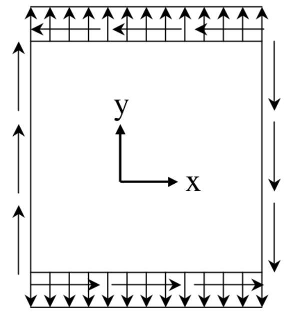
Tension/Negative Shear	$N_{y,max}/N_{xy,max} = 2.0$	TNS_2	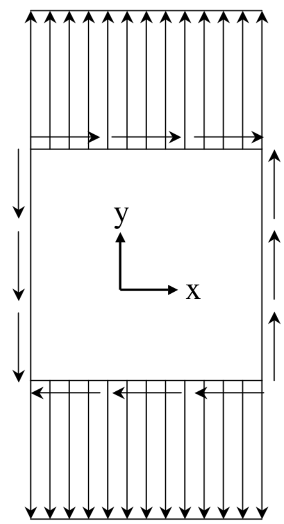
Tension/Negative Shear	$N_{y,max}/N_{xy,max} = 1.0$	TNS_1	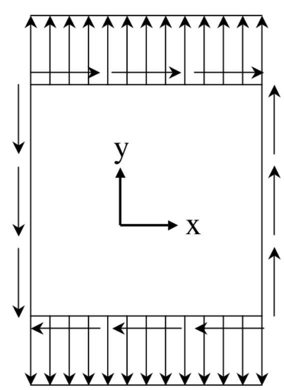
Tension/Negative Shear	$N_{y,max}/N_{xy,max} = 0.5$	TNS_05	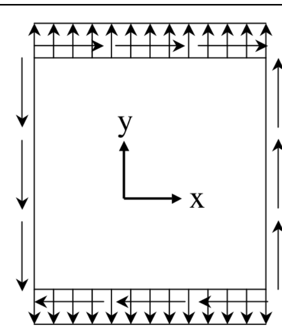

Table 9 (cont.): Load case definitions

Load Condition Type	Ratio	Designation	Representation
Tension/In-Plane Bending	$N_{y,max}/N_{x,max} = 1.0$	TB1_1	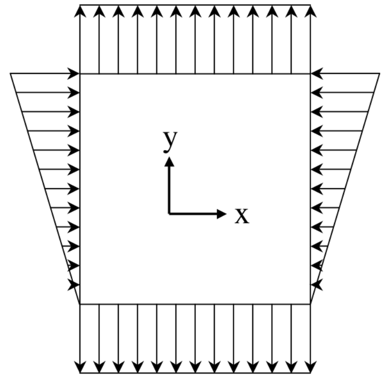
Tension/In-Plane Bending	$N_{y,max}/N_{x,max} = 0.5$	TB1_05	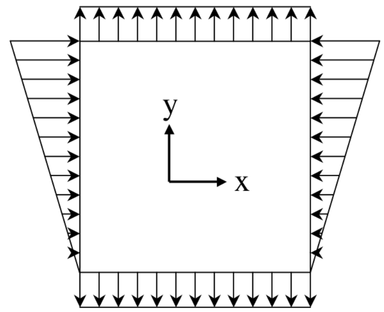
Tension/In-Plane Bending	$N_{y,max}/N_{x,max} = 1.0$	TB2_1	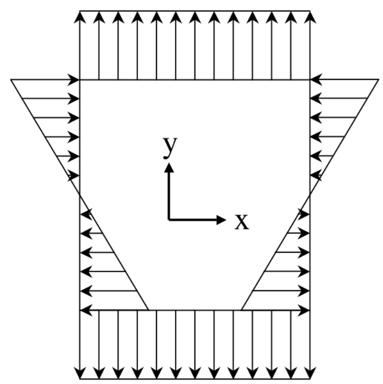
Tension/In-Plane Bending	$N_{y,max}/N_{x,max} = 0.5$	TB2_05	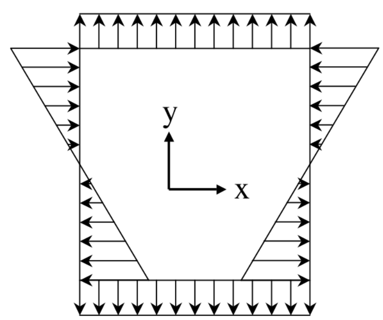

Table 10: Analysis matrix for flat, square panels under combined loads

Load Case	Buckling		Strength	
	Dimensions (in.)	Sequence	Dimensions (in.)	Sequence
TC	5, 14, 21, 28	$[45/-45/0/90]_{ns}$ n = 1,2,3,4,5,6	5, 8, 10, 14	$[45/-45/0/90]_{ns}$ n = 1,2,3,4,5,6,7
	Dimensions (in.)	Sequence	Dimensions (in.)	Sequence
TS_2	5, 14, 21, 28	$[45/-45/0/90]_{ns}$ n = 1,2,3,4,5,6	5, 8, 10, 14	$[45/-45/0/90]_{ns}$ n = 1,2,3,4,5,6,7
	Dimensions (in.)	Sequence	Dimensions (in.)	Sequence
TS_1	5, 14, 21, 28	$[45/-45/0/90]_{ns}$ n = 1,2,3,4,5,6	5, 8, 10, 14	$[45/-45/0/90]_{ns}$ n = 1,2,3,4,5,6,7
	Dimensions (in.)	Sequence	Dimensions (in.)	Sequence
TS_05	5, 14, 21, 28	$[45/-45/0/90]_{ns}$ n = 1,2,3,4,5,6	5, 8, 10, 14	$[45/-45/0/90]_{ns}$ n = 1,2,3,4,5,6,7
	Dimensions (in.)	Sequence		
TNS_2	5, 14, 21, 28	$[45/-45/0/90]_{ns}$ n = 1,2,3,4,5,6		
	Dimensions (in.)	Sequence		
TNS_1	5, 14, 21, 28	$[45/-45/0/90]_{ns}$ n = 1,2,3,4,5,6		
	Dimensions (in.)	Sequence		
TNS_05	5, 14, 21, 28	$[45/-45/0/90]_{ns}$ n = 1,2,3,4,5,6		
	Dimensions (in.)	Sequence		
TB1_1	5, 14, 21, 28	$[45/-45/0/90]_{ns}$ n = 1,2,3,4,5,6		
	Dimensions (in.)	Sequence		
TB1_05	5, 14, 21, 28	$[45/-45/0/90]_{ns}$ n = 1,2,3,4,5,6		
	Dimensions (in.)	Sequence		
TB2_1	5, 14, 21, 28	$[45/-45/0/90]_{ns}$ n = 1,2,3,4,5,6		
	Dimensions (in.)	Sequence		
TB2_05	5, 14, 21, 28	$[45/-45/0/90]_{ns}$ n = 1,2,3,4,5,6		

Table 11: Buckling analysis actuator forces for load case TC

	Tension Actuator Force (lbs.)				Compression Actuator Force (lbs.)			
# Plies	5 in.	14 in.	21 in.	28 in.	5 in.	14 in.	21 in.	28 in.
8	874	314	209	157	874	314	209	157
16	7199	2584	1723	1292	7199	2584	1723	1292
24	24275	8714	5809	4357	24275	8714	5809	4357
32	57413	20609	13739	10305	57413	20609	13739	10305
40	111920	40175	26783	20088	111920	40175	26783	20088
48	193106	69318	46212	34659	193106	69318	46212	34659

Table 12: Buckling analysis actuator forces for load case TS_2

	Tension Actuator Force (lbs.)				Shear Actuator Force (lbs.)			
# Plies	5 in.	14 in.	21 in.	28 in.	5 in.	14 in.	21 in.	28 in.
8	12633	3154	2103	1577	6317	1577	1051	789
16	91327	28057	18704	14028	45664	14028	9352	7014
24	296820	96492	64328	48246	148410	48246	32164	24123
32	689895	230242	153495	115121	344948	115121	76747	57561
40	1331335	451093	300729	225547	665668	225547	150364	112773
48	2281922	780826	520551	390413	1140961	390413	260275	195206

Table 13: Buckling analysis actuator forces for load case TS_1

	Tension Actuator Force (lbs.)				Shear Actuator Force (lbs.)			
# Plies	5 in.	14 in.	21 in.	28 in.	5 in.	14 in.	21 in.	28 in.
8	2848	680	454	340	2848	680	454	340
16	20100	6017	4011	3008	20100	6017	4011	3008
24	64926	20696	13798	10348	64926	20696	13798	10348
32	150505	49404	32936	24702	150505	49404	32936	24702
40	290017	96826	64550	48413	290017	96826	64550	48413
48	496640	167646	111764	83823	496640	167646	111764	83823

Table 14: Buckling analysis actuator forces for load case TS_05

	Tension Actuator Force (lbs.)				Shear Actuator Force (lbs.)			
# Plies	5 in.	14 in.	21 in.	28 in.	5 in.	14 in.	21 in.	28 in.
8	898	211	141	106	1796	422	281	211
16	6301	1873	1249	937	12603	3746	2497	1873
24	20370	6465	4310	1616	40739	12930	8620	3233
32	47265	15467	10311	7733	94530	30933	20622	15467
40	91150	30357	20238	15178	182300	60714	40476	30357
48	156184	52615	35077	26307	312369	105230	70153	52615

Table 15: Buckling analysis actuator forces for load case TSN_2

	Tension Actuator Force (lbs.)				Shear Actuator Force (lbs.)			
# Plies	5 in.	14 in.	21 in.	28 in.	5 in.	14 in.	21 in.	28 in.
8	8806	4525	3016	2262	4403	2262	1508	1131
16	78309	32715	21810	16358	39155	16358	10905	8179
24	269298	106340	70893	53170	134649	53170	35447	26585
32	642554	247181	164787	123591	321277	123591	82394	61795
40	1258862	477023	318015	238512	629431	238512	159008	119256
48	2179003	817648	545099	408824	1089502	408824	272549	204412

Table 16: Buckling analysis actuator forces for load case TSN_1

	Tension Actuator Force (lbs.)				Shear Actuator Force (lbs.)			
# Plies	5 in.	14 in.	21 in.	28 in.	5 in.	14 in.	21 in.	28 in.
8	1915	1012	675	506	1915	1012	675	506
16	16930	7144	4763	3572	16930	7144	4763	3572
24	58229	23077	15385	11539	58229	23077	15385	11539
32	138989	53498	35665	26749	138989	53498	35665	26749
40	272391	103091	68727	51546	272391	103091	68727	51546
48	471613	176542	117695	88271	471613	176542	117695	88271

Table 17: Buckling analysis actuator forces for load case TSN_05

	Tension Actuator Force (lbs.)				Shear Actuator Force (lbs.)			
# Plies	5 in.	14 in.	21 in.	28 in.	5 in.	14 in.	21 in.	28 in.
8	594	319	213	160	1189	638	425	319
16	5271	2239	1493	1119	10543	4478	2985	2239
24	18194	7238	4825	3619	36387	14476	9651	7238
32	43523	16796	11197	8398	87047	33591	22394	16796
40	85422	32394	21595	16195	170845	64788	43190	32391
48	148053	55503	37002	27752	296105	111006	74004	55503

Table 18: Buckling analysis actuator forces for load case TB1_1

	Tension Actuator Force (lbs.)				Compression Actuator Force (lbs.) (+/0)			
# Plies	5 in.	14 in.	21 in.	28 in.	5 in.	14 in.	21 in.	28 in.
8	2100	750	500	375	2100	750	500	375
16	17318	6185	4123	3092	17318	6185	4123	3092
24	58446	20874	13916	10437	58446	20874	13916	10437
32	138300	49393	32929	24696	138300	49393	32929	24696
40	269691	96318	64212	48159	269691	96318	64212	48159
48	465433	166226	110817	83113	465433	166226	110817	83113

Table 19: Buckling analysis actuator forces for load case TB1_05

	Tension Actuator Force (lbs.)				Compression Actuator Force (lbs.) (+/0)			
# Plies	5 in.	14 in.	21 in.	28 in.	5 in.	14 in.	21 in.	28 in.
8	812	290	193	145	1623	580	386	290
16	6672	2383	1589	1191	13344	4766	3177	2383
24	22491	8032	5355	4016	44982	16065	10710	8032
32	53188	18996	12664	9498	106375	37991	25327	18996
40	103681	37029	24686	18514	207361	74058	49372	37029
48	178889	63889	42593	31944	357778	127778	85185	63889

Table 20: Buckling analysis actuator forces for load case TB2_1

	Tension Actuator Force (lbs.)				Compression Actuator Force (lbs.) (+/0)			
# Plies	5 in.	14 in.	21 in.	28 in.	5 in.	14 in.	21 in.	28 in.
8	5831	2082	1388	1041	2915	1041	694	521
16	47991	17140	11427	8570	23996	8570	5713	4285
24	161853	57805	38537	28902	80927	28902	19268	14451
32	382847	136731	91154	68366	191424	68366	45577	34183
40	746499	266607	177738	133303	373250	133303	88869	66652
48	1287941	459979	306653	229990	643971	229990	153326	114995

Table 21: Buckling analysis actuator forces for load case TB2_05

	Tension Actuator Force (lbs.)				Compression Actuator Force (lbs.) (+/-)			
# Plies	5 in.	14 in.	21 in.	28 in.	5 in.	14 in.	21 in.	28 in.
8	2227	795	530	398	2227	795	530	398
16	18182	6493	4329	3247	18182	6493	4329	3247
24	61199	21857	14571	10928	61199	21857	14571	10928
32	144643	51658	34439	25829	144643	51658	34439	25829
40	281874	100669	67113	50335	281874	100669	67113	50335
48	486254	173662	115775	86831	486254	173662	115775	86831

Table 22: Buckling analysis actuator strokes for load case TC

	Tension Actuator Stroke (in.)				Compression Actuator Stroke (in.)			
# Plies	5 in.	14 in.	21 in.	28 in.	5 in.	14 in.	21 in.	28 in.
8	0.007182	0.002549	0.001699	0.001274	0.006942	0.002488	0.001658	0.001244
16	0.02958	0.01050	0.006997	0.005248	0.02859	0.01024	0.006829	0.005122
24	0.06650	0.02359	0.01573	0.01180	0.06427	0.02303	0.01535	0.01151
32	0.1180	0.04185	0.02790	0.02092	0.1140	0.04084	0.02723	0.02042
40	0.1839	0.06527	0.04351	0.03263	0.1778	0.06370	0.04246	0.03185
48	0.2645	0.09384	0.06256	0.04692	0.2556	0.09158	0.06106	0.04579

Table 23: Buckling analysis actuator strokes for load case TS_2

	Tension Actuator Stroke (in.)				Shear Actuator Stroke (in.)			
# Plies	5 in.	14 in.	21 in.	28 in.	5 in.	14 in.	21 in.	28 in.
8	0.07907	0.01946	0.01297	0.00973	0.09992	0.02495	0.01663	0.01247
16	0.2858	0.08655	0.05770	0.04327	0.3612	0.1110	0.0740	0.0555
24	0.6193	0.1984	0.1323	0.0992	0.7826	0.2544	0.1696	0.1272
32	1.080	0.3551	0.2367	0.1776	1.364	0.4553	0.3035	0.2276
40	1.667	0.5566	0.3711	0.2783	2.106	0.7136	0.4757	0.3568
48	2.380	0.8029	0.5352	0.4014	3.008	1.029	0.686	0.515

Table 24: Buckling analysis actuator strokes for load case TS_1

	Tension Actuator Stroke (in.)				Shear Actuator Stroke (in.)			
# Plies	5 in.	14 in.	21 in.	28 in.	5 in.	14 in.	21 in.	28 in.
8	0.01783	0.004197	0.002798	0.002098	0.04505	0.01076	0.00717	0.00538
16	0.06290	0.01856	0.01237	0.00928	0.1590	0.04759	0.03173	0.02380
24	0.1355	0.04256	0.02837	0.02128	0.3424	0.1091	0.0728	0.0546
32	0.2355	0.07620	0.05080	0.03810	0.5952	0.1954	0.1303	0.0977
40	0.3630	0.1195	0.0796	0.0597	0.9175	0.3063	0.2042	0.1532
48	0.5181	0.1724	0.1149	0.0862	1.309	0.4420	0.2947	0.2210

Table 25: Buckling analysis actuator strokes for load case TS_05

	Tension Actuator Stroke (in.)				Shear Actuator Stroke (in.)			
# Plies	5 in.	14 in.	21 in.	28 in.	5 in.	14 in.	21 in.	28 in.
8	0.005621	0.001302	0.000868	0.000651	0.02841	0.006679	0.004453	0.003340
16	0.01972	0.005778	0.003852	0.002889	0.09968	0.02963	0.01975	0.01481
24	0.04250	0.01330	0.00886	0.00332	0.2148	0.06818	0.04545	0.01705
32	0.07396	0.02386	0.01590	0.01193	0.3738	0.1223	0.0816	0.0612
40	0.1141	0.03746	0.02497	0.01873	0.5768	0.1921	0.1281	0.0960
48	0.1629	0.05410	0.03607	0.02705	0.8236	0.2774	0.1850	0.1387

Table 26: Buckling analysis actuator strokes for load case TSN_2

	Tension Actuator Stroke (in.)				Shear Actuator Stroke (in.)			
# Plies	5 in.	14 in.	21 in.	28 in.	5 in.	14 in.	21 in.	28 in.
8	0.05512	0.02791	0.01861	0.01396	0.06965	0.03579	0.02386	0.01789
16	0.2451	0.1009	0.0673	0.0505	0.3097	0.1294	0.0863	0.0647
24	0.5618	0.2187	0.1458	0.1093	0.7100	0.2804	0.1869	0.1402
32	1.005	0.3812	0.2542	0.1906	1.271	0.4888	0.3258	0.2444
40	1.576	0.5886	0.3924	0.2943	1.991	0.7546	0.5031	0.3773
48	2.273	0.8407	0.5605	0.4204	2.872	1.078	0.719	0.539

Table 27: Buckling analysis actuator strokes for load case TSN_1

	Tension Actuator Stroke (in.)				Shear Actuator Stroke (in.)			
# Plies	5 in.	14 in.	21 in.	28 in.	5 in.	14 in.	21 in.	28 in.
8	0.01198	0.006245	0.004163	0.003122	0.03029	0.01601	0.01067	0.00801
16	0.05298	0.02204	0.01469	0.01102	0.1339	0.05650	0.03767	0.02825
24	0.1215	0.04746	0.03164	0.02373	0.3070	0.1217	0.0811	0.0608
32	0.2175	0.08251	0.05501	0.04126	0.5497	0.2116	0.1410	0.1058
40	0.3410	0.1272	0.0848	0.0636	0.8618	0.3262	0.2174	0.1631
48	0.4920	0.1815	0.1210	0.0908	1.243	0.4654	0.3103	0.2327

Table 28: Buckling analysis actuator strokes for load case TSN_05

	Tension Actuator Stroke (in.)				Shear Actuator Stroke (in.)			
# Plies	5 in.	14 in.	21 in.	28 in.	5 in.	14 in.	21 in.	28 in.
8	0.00372	0.001968	0.001312	0.000984	0.01880	0.01009	0.00673	0.00505
16	0.01650	0.006906	0.004604	0.003453	0.08339	0.03542	0.02361	0.01771
24	0.03796	0.01489	0.00992	0.00744	0.1919	0.07633	0.05089	0.03817
32	0.06810	0.02590	0.01727	0.01295	0.3442	0.1328	0.0886	0.0664
40	0.1069	0.03997	0.02665	0.01998	0.5405	0.2050	0.1366	0.1025
48	0.1544	0.05707	0.03805	0.02854	0.7807	0.2927	0.1951	0.1463

Table 29: Buckling analysis actuator strokes for load case TB1_1

	Tension Actuator Stroke (in.)				Compression Actuator Stroke (in.) (+/0)			
# Plies	5 in.	14 in.	21 in.	28 in.	5 in.	14 in.	21 in.	28 in.
8	0.01522	0.005434	0.002415	0.001359	0.01672	0.005970	0.002653	0.001493
16	0.06274	0.02241	0.009959	0.005602	0.06893	0.02462	0.01094	0.006155
24	0.1293	0.04617	0.02052	0.01154	0.1551	0.05539	0.02462	0.01385
32	0.2505	0.08947	0.03977	0.02237	0.2752	0.09830	0.04369	0.02458
40	0.3908	0.1396	0.06204	0.03490	0.4294	0.1534	0.06816	0.03834
48	0.5621	0.2007	0.08922	0.05019	0.6175	0.2205	0.09802	0.05514

Table 30: Buckling analysis actuator strokes for load case TB1_05

	Tension Actuator Stroke (in.)				Compression Actuator Stroke (in.) (+/0)			
# Plies	5 in.	14 in.	21 in.	28 in.	5 in.	14 in.	21 in.	28 in.
8	0.006755	0.002412	0.001072	0.0006031	0.01132	0.004044	0.001798	0.001011
16	0.02776	0.009915	0.004407	0.002479	0.04655	0.01662	0.007388	0.004156
24	0.06239	0.02228	0.009903	0.005571	0.1046	0.03736	0.01660	0.009340
32	0.1107	0.03952	0.01757	0.009880	0.1855	0.06626	0.02945	0.01656
40	0.1726	0.06163	0.02739	0.01541	0.2893	0.1033	0.04592	0.02583
48	0.2481	0.08862	0.03939	0.02215	0.4160	0.1486	0.06603	0.03714

Table 31: Buckling analysis actuator strokes for load case TB2_1

	Tension Actuator Stroke (in.)				Compression Actuator Stroke (in.) (+/-)			
# Plies	5 in.	14 in.	21 in.	28 in.	5 in.	14 in.	21 in.	28 in.
8	0.03597	0.01285	0.005710	0.003212	0.04646	0.01659	0.007374	0.004148
16	0.1480	0.05287	0.02350	0.01322	0.1912	0.06828	0.030346	0.01707
24	0.3328	0.1189	0.05283	0.02972	0.4298	0.1535	0.068228	0.03838
32	0.5905	0.2109	0.09373	0.05272	0.7626	0.2723	0.1210	0.06809
40	0.9211	0.3290	0.1462	0.08224	1.190	0.4248	0.1888	0.1062
48	1.324	0.4730	0.2102	0.1182	1.710	0.6108	0.2715	0.1527

Table 32: Buckling analysis actuator strokes for load case TB2_05

	Tension Actuator Stroke (in.)				Compression Actuator Stroke (in.) (+/-)			
# Plies	5 in.	14 in.	21 in.	28 in.	5 in.	14 in.	21 in.	28 in.
8	0.01374	0.004907	0.002181	0.001227	0.03110	0.01111	0.004937	0.002777
16	0.05609	0.02003	0.008902	0.005008	0.1270	0.04534	0.02015	0.01134
24	0.1259	0.04495	0.01998	0.01124	0.2849	0.1017	0.04522	0.02544
32	0.2231	0.07968	0.03541	0.01992	0.5050	0.1804	0.08016	0.04509
40	0.3478	0.1242	0.05521	0.03105	0.7873	0.2812	0.1250	0.07029
48	0.5000	0.1786	0.07936	0.04464	1.132	0.4042	0.1797	0.1011

Table 33: Strength analysis actuator forces for load case TC

	Tension Actuator Force (lbs.)				Compression Actuator Force (lbs.)			
# Plies	5 in.	8 in.	10 in.	14 in.	5 in.	8 in.	10 in.	14 in.
8	4606	7370	9212	12897	4606	7370	9212	12897
16	18424	29479	36848	51587	18424	29479	36848	51587
24	41454	66327	82908	116072	41454	66327	82908	116072
32	73696	117914	147393	206350	73696	117914	147393	206350
40	115151	184241	230301	322422	115151	184241	230301	322422
48	165817	265307	331633	464286	165817	265307	331633	464286
56	225695	361112	451390	631946	225695	361112	451390	631946

Table 34: Strength analysis actuator forces for load case TS_2

	Tension Actuator Force (lbs.)				Shear Actuator Force (lbs.)			
# Plies	5 in.	8 in.	10 in.	14 in.	5 in.	8 in.	10 in.	14 in.
8	5525	8840	11050	15470	5525	8840	11050	15470
16	22100	35360	44200	61880	22100	35360	44200	61880
24	49725	79560	99449	139229	49725	79560	99449	139229
32	88400	141439	176799	247519	88400	141439	176799	247519
40	138125	220999	276249	386749	138125	220999	276249	386749
48	198899	318238	397798	556917	198899	318238	397798	556917
56	270723	433157	541447	758025	270723	433157	541447	758025

Table 35: Strength analysis actuator forces for load case TS_1

	Tension Actuator Force (lbs.)				Shear Actuator Force (lbs.)			
# Plies	5 in.	8 in.	10 in.	14 in.	5 in.	8 in.	10 in.	14 in.
8	2373	3797	4746	6644	2373	3797	4746	6644
16	9492	15187	18984	26577	9492	15187	18984	26577
24	21357	34171	42713	59798	21357	34171	42713	59798
32	37967	60747	75934	106308	37967	60747	75934	106308
40	59324	94918	118647	166106	59324	94918	118647	166106
48	85426	136682	170852	239193	85426	136682	170852	239193
56	116274	186039	232548	325568	116274	186039	232548	325568

Table 36: Strength analysis actuator forces for load case TS_05

	Tension Actuator Force (lbs.)				Shear Actuator Force (lbs.)			
# Plies	5 in.	8 in.	10 in.	14 in.	5 in.	8 in.	10 in.	14 in.
8	815	1304	1630	2282	1630	2608	3260	4564
16	3260	5216	6520	9128	6520	10432	13040	18256
24	7335	11736	14670	20537	14670	23471	29339	41075
32	13040	20863	26079	36511	26079	41727	52159	73022
40	20374	32599	40749	57048	40749	65198	81498	114097
48	29339	46943	58678	82149	58678	93885	117356	164299
56	39934	63894	79868	111815	79868	127789	159736	223630

Table 37: Strength analysis actuator strokes for load case TC

	Tension Actuator Stroke (in.)				Compression Actuator Stroke (in.)			
# Plies	5 in.	8 in.	10 in.	14 in.	5 in.	8 in.	10 in.	14 in.
8	0.03785	0.1696	0.3179	0.5935	0.03658	0.1639	0.3073	0.5736
16	0.07570	0.3391	0.6359	1.187	0.07316	0.3278	0.6146	1.147
24	0.1136	0.5087	0.9538	1.781	0.1097	0.4917	0.9219	1.721
32	0.1514	0.6783	1.272	2.374	0.1463	0.6556	1.229	2.294
40	0.1893	0.8479	1.590	2.968	0.1829	0.8194	1.536	2.868
48	0.2271	1.017	1.908	3.561	0.2195	0.9833	1.844	3.442
56	0.2650	1.187	2.226	4.155	0.2561	1.147	2.151	4.015

Table 38: Strength analysis actuator strokes for load case TS_2

	Tension Actuator Stroke (in.)				Shear Actuator Stroke (in.)			
# Plies	5 in.	8 in.	10 in.	14 in.	5 in.	8 in.	10 in.	14 in.
8	0.03458	0.1549	0.2905	0.5422	0.04370	0.1958	0.3671	0.6852
16	0.06916	0.3098	0.5810	1.084	0.08740	0.3915	0.7341	1.370
24	0.1037	0.4648	0.8714	1.627	0.1311	0.5873	1.101	2.056
32	0.1383	0.6197	1.162	2.169	0.1748	0.7831	1.468	2.741
40	0.1729	0.7746	1.452	2.711	0.2185	0.9789	1.835	3.426
48	0.2075	0.9295	1.743	3.253	0.2622	1.175	2.202	4.111
56	0.2421	1.084	2.033	3.796	0.3059	1.370	2.570	4.796

Table 39: Strength analysis actuator strokes for load case TS_1

	Tension Actuator Stroke (in.)				Shear Actuator Stroke (in.)			
# Plies	**5 in.**	**8 in.**	**10 in.**	**14 in.**	**5 in.**	**8 in.**	**10 in.**	**14 in.**
8	0.01485	0.06654	0.1248	0.2329	0.03754	0.1682	0.3153	0.5886
16	0.02970	0.1331	0.2495	0.4658	0.07507	0.3363	0.6306	1.177
24	0.04456	0.1996	0.3743	0.6987	0.1126	0.5045	0.9459	1.766
32	0.05941	0.2662	0.4990	0.9315	0.1501	0.6727	1.261	2.354
40	0.07426	0.3327	0.6238	1.164	0.1877	0.8408	1.577	2.943
48	0.08911	0.3992	0.7486	1.397	0.2252	1.009	1.892	3.531
56	0.1040	0.4658	0.8733	1.630	0.2628	1.177	2.207	4.120

Table 40: Strength analysis actuator strokes for load case TS_05

	Tension Actuator Stroke (in.)				Shear Actuator Stroke (in.)			
# Plies	**5 in.**	**8 in.**	**10 in.**	**14 in.**	**5 in.**	**8 in.**	**10 in.**	**14 in.**
8	0.005101	0.02285	0.04285	0.07998	0.02578	0.1155	0.2166	0.4043
16	0.01020	0.04570	0.08570	0.1600	0.05157	0.2310	0.4332	0.8086
24	0.01530	0.06856	0.1285	0.2399	0.07735	0.3465	0.6498	1.213
32	0.02040	0.09141	0.1714	0.3199	0.1031	0.4620	0.8663	1.617
40	0.02550	0.1143	0.2142	0.3999	0.1289	0.5776	1.083	2.021
48	0.03061	0.1371	0.2571	0.4799	0.1547	0.6931	1.300	2.426
56	0.03571	0.1600	0.2999	0.5599	0.1805	0.8086	1.516	2.830

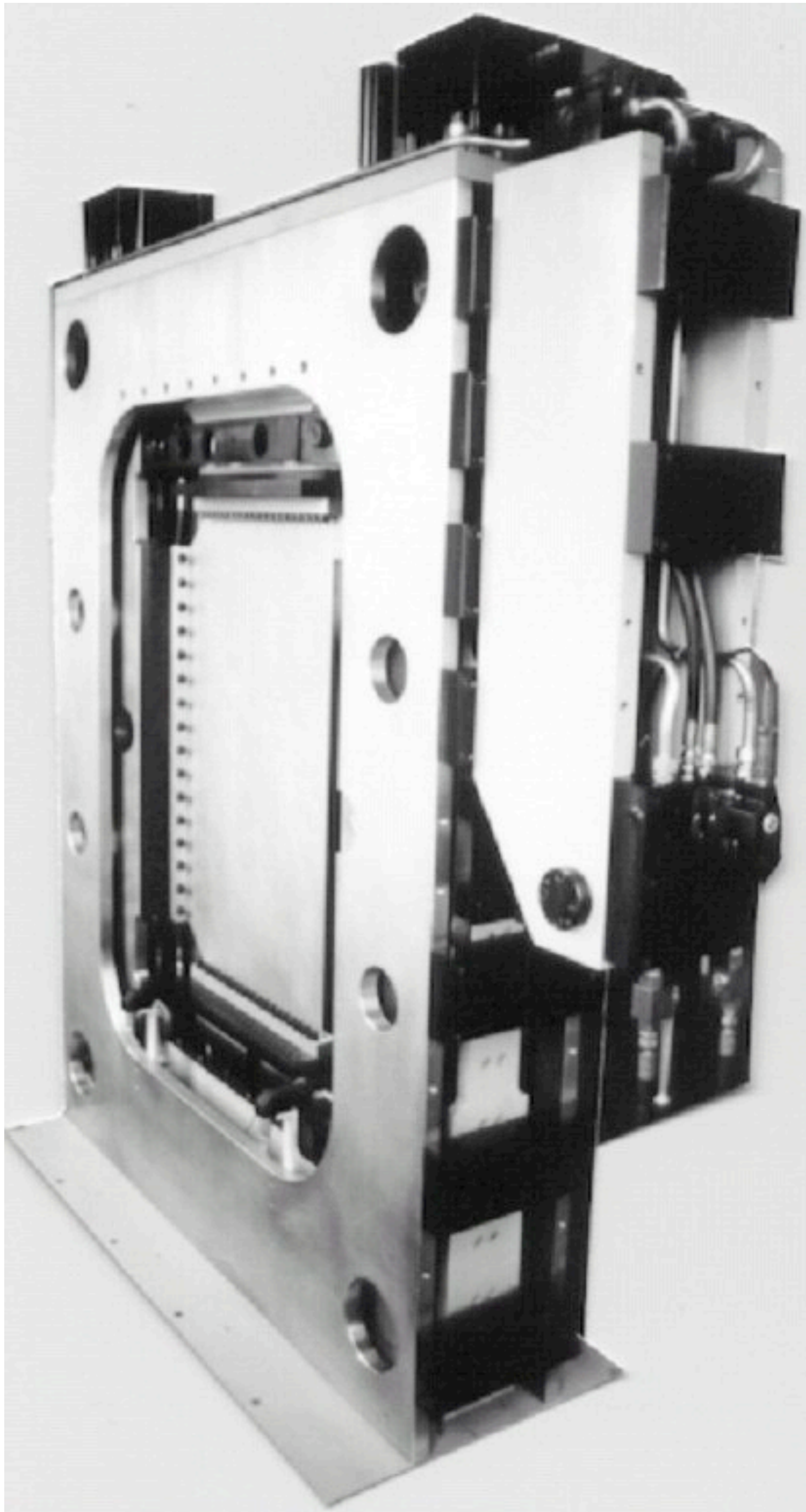

Figure 11: Combined-loads test machine of References 4 – 8 (used with permission)

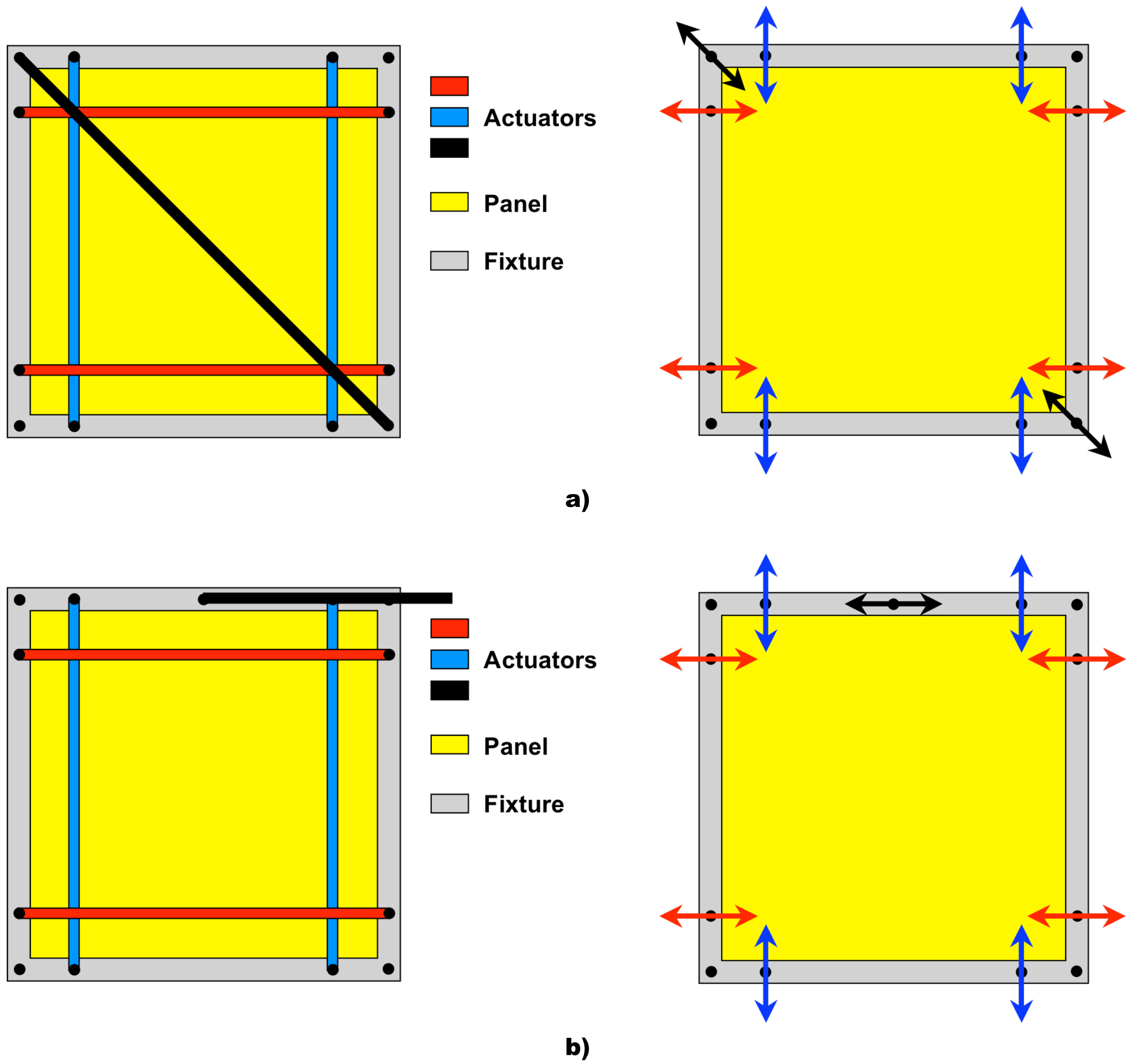

Figure 12: Proposed NASA LaRC combined-load test configurations

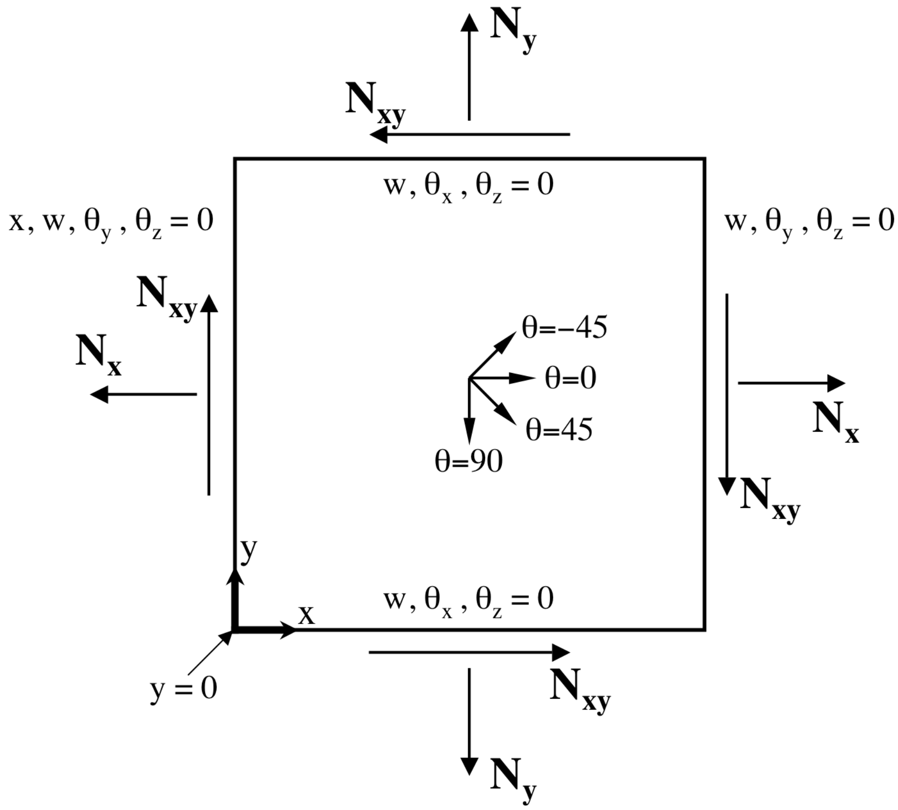

Figure 13: Panel definition and boundary conditions

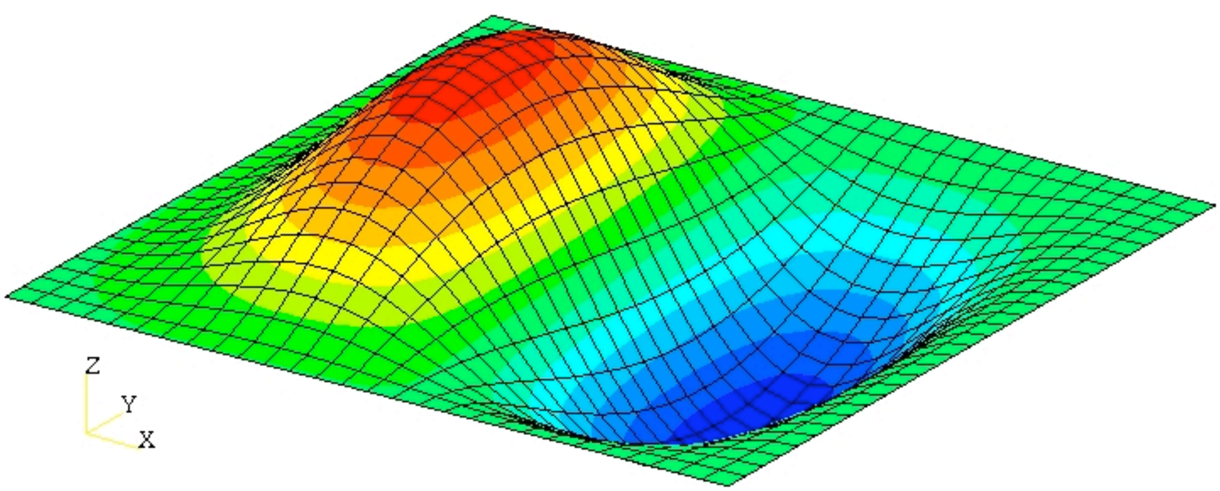

Figure 14: Fundamental mode shape for load case TC

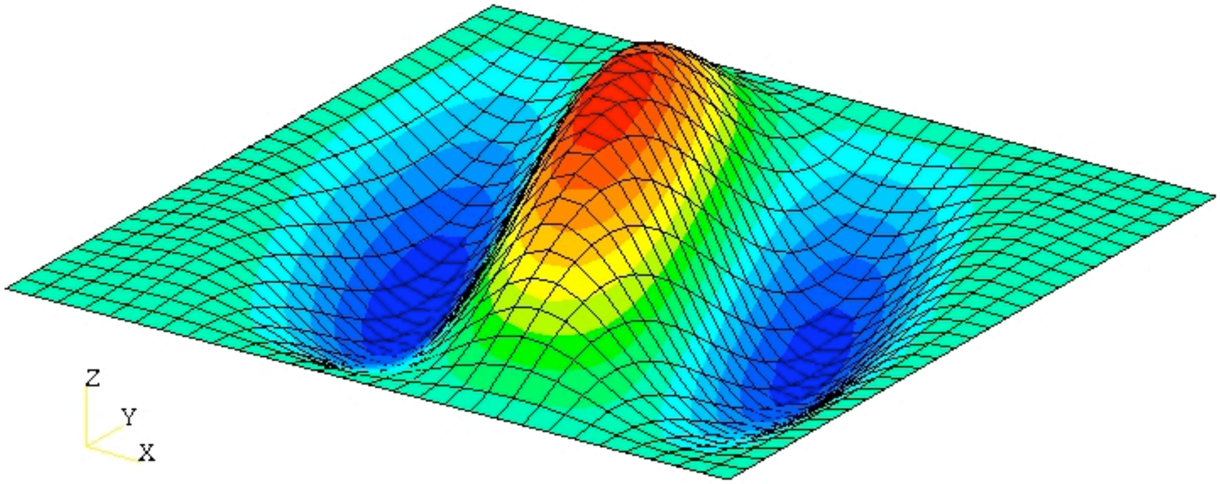

Figure 15: Fundamental mode shape for load case TS_2

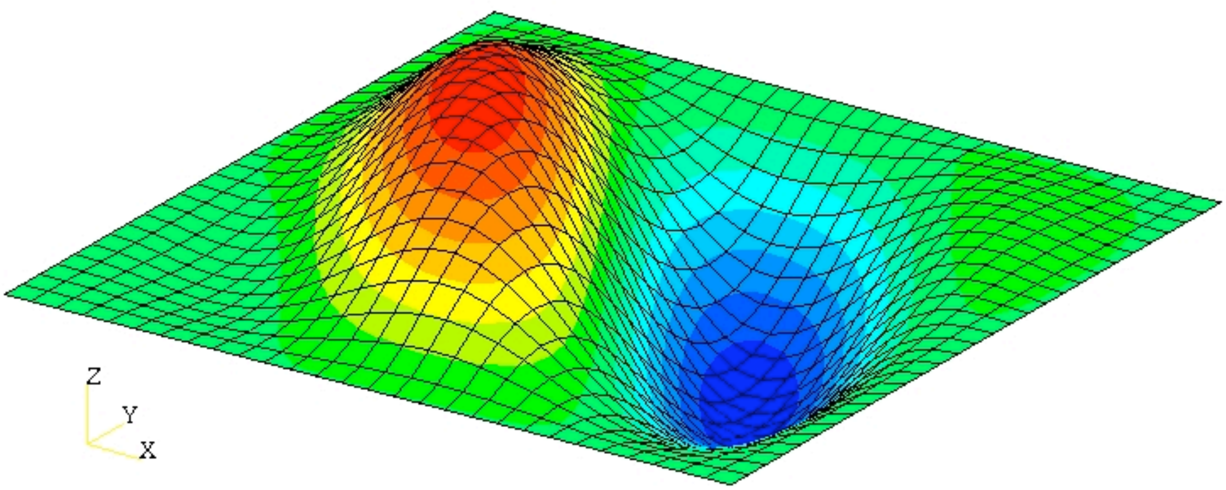

Figure 16: Fundamental mode shape for load case TS_1

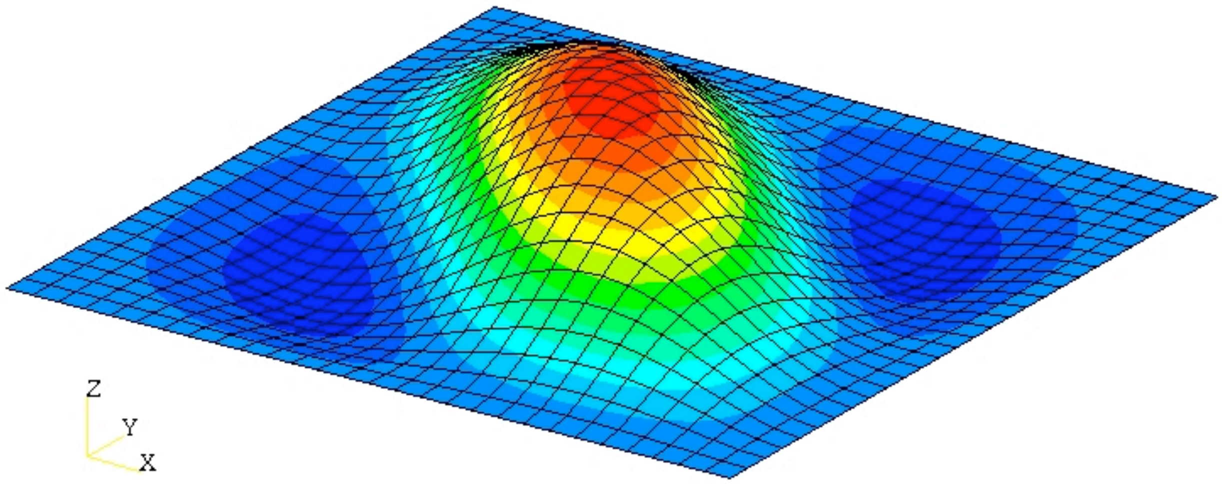

Figure 17: Fundamental mode shape for load case TS_05

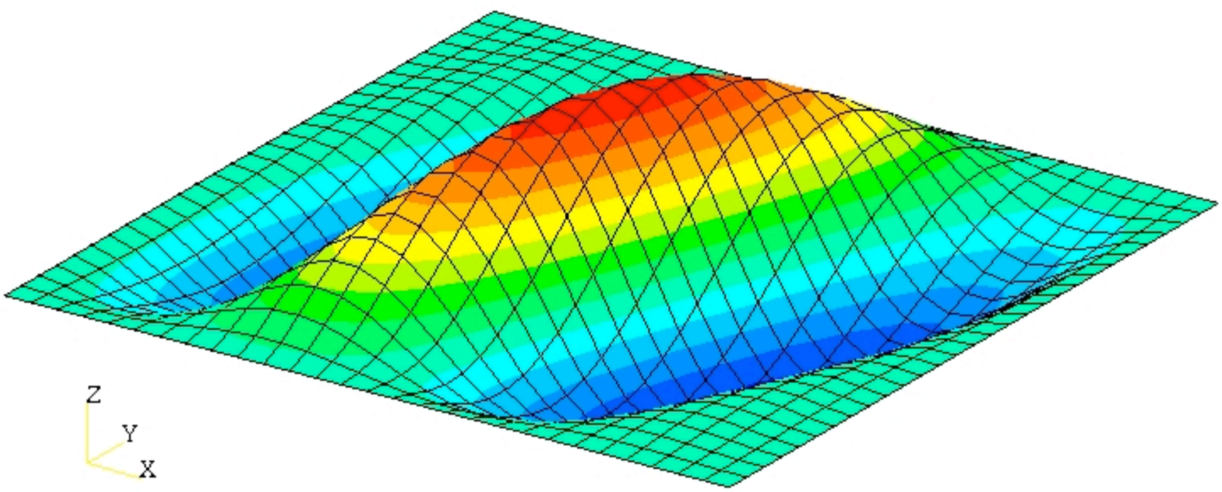

Figure 18: Fundamental mode shape for load case TSN_2

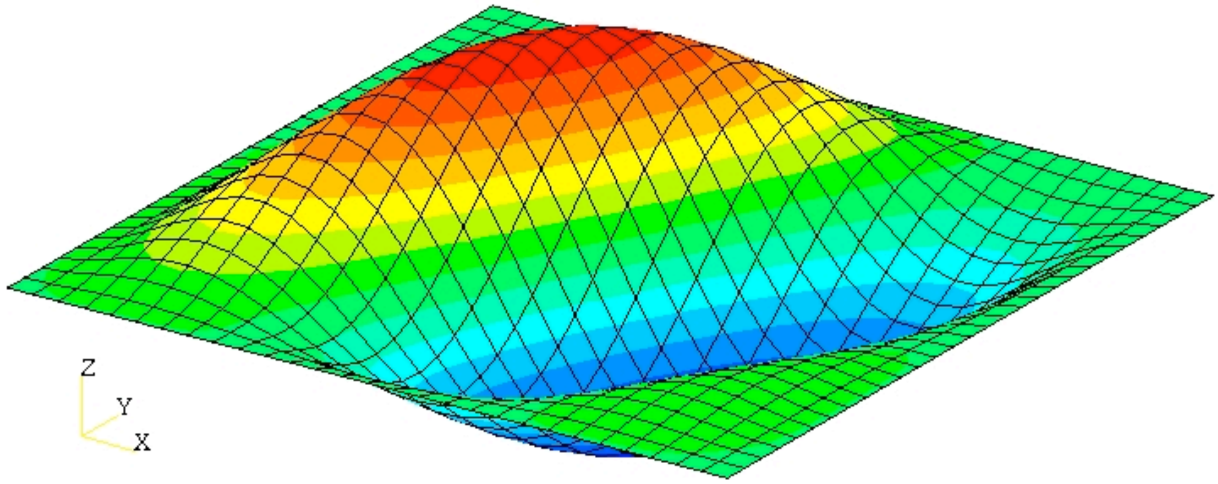

Figure 19: Fundamental mode shape for load case TSN_1

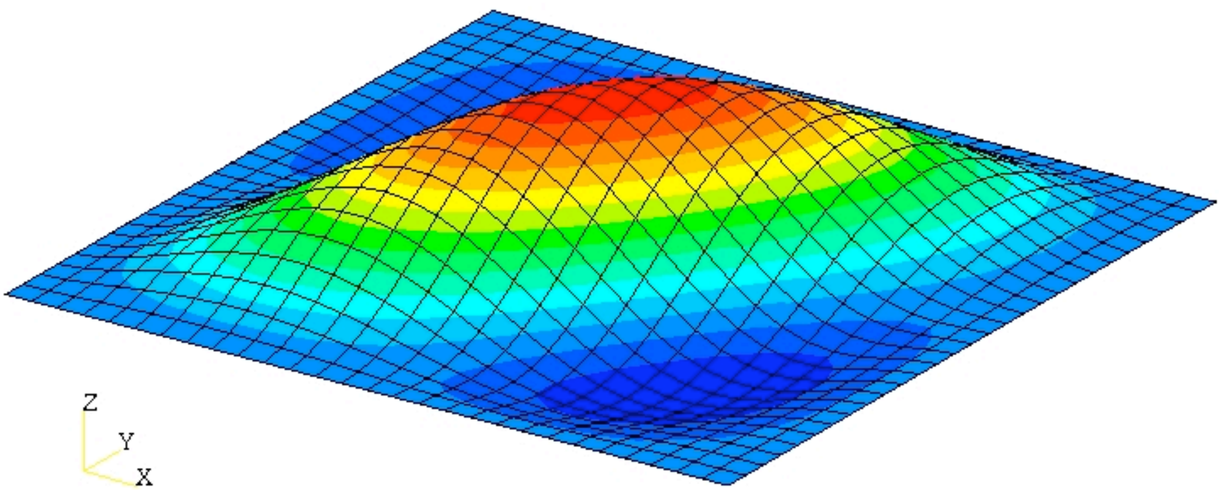

Figure 20: Fundamental mode shape for load case TSN_05

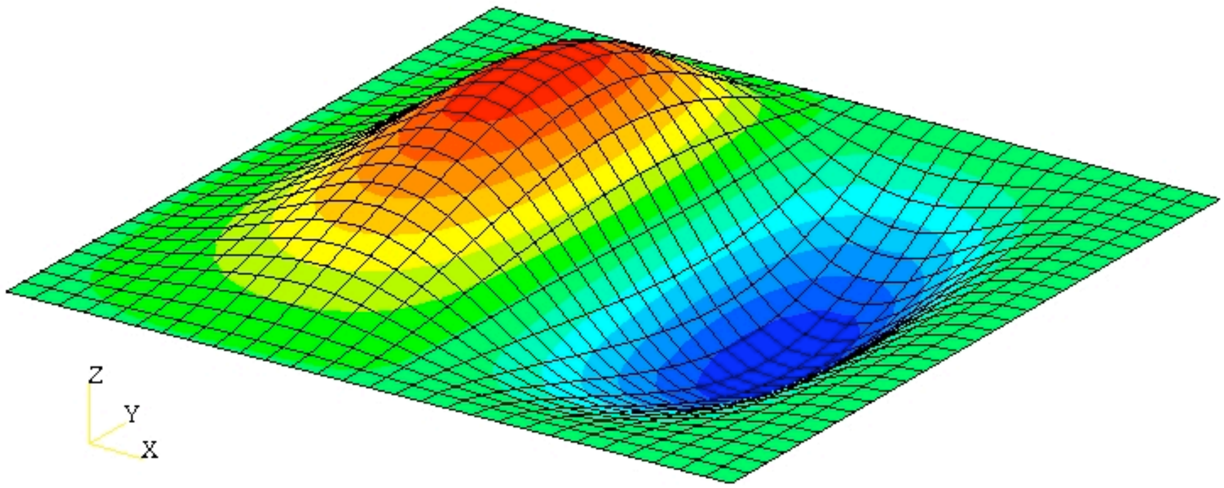

Figure 21: Fundamental mode shape for load case TB1_1

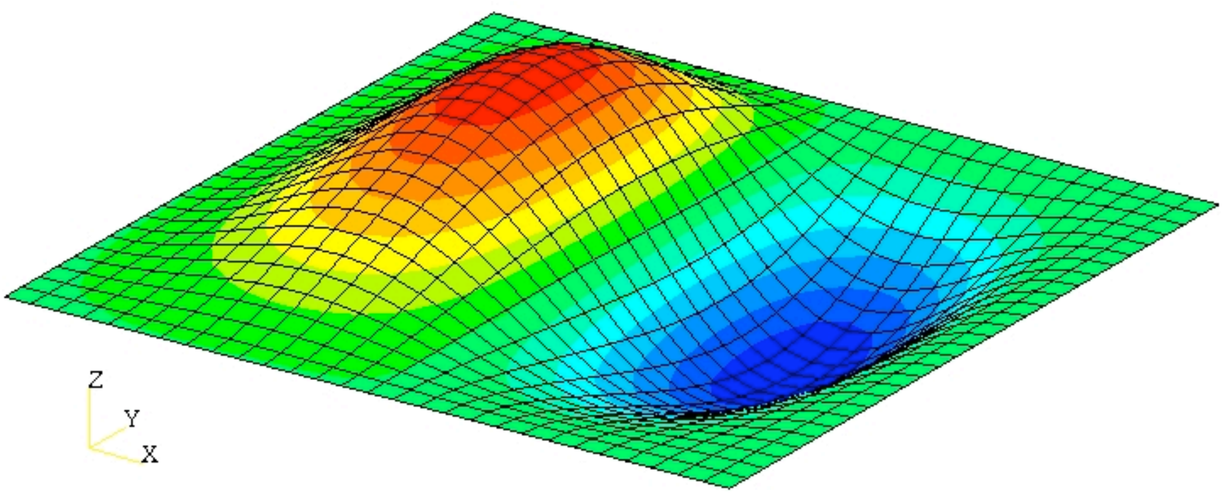

Figure 22: Fundamental mode shape for load case TB1_05

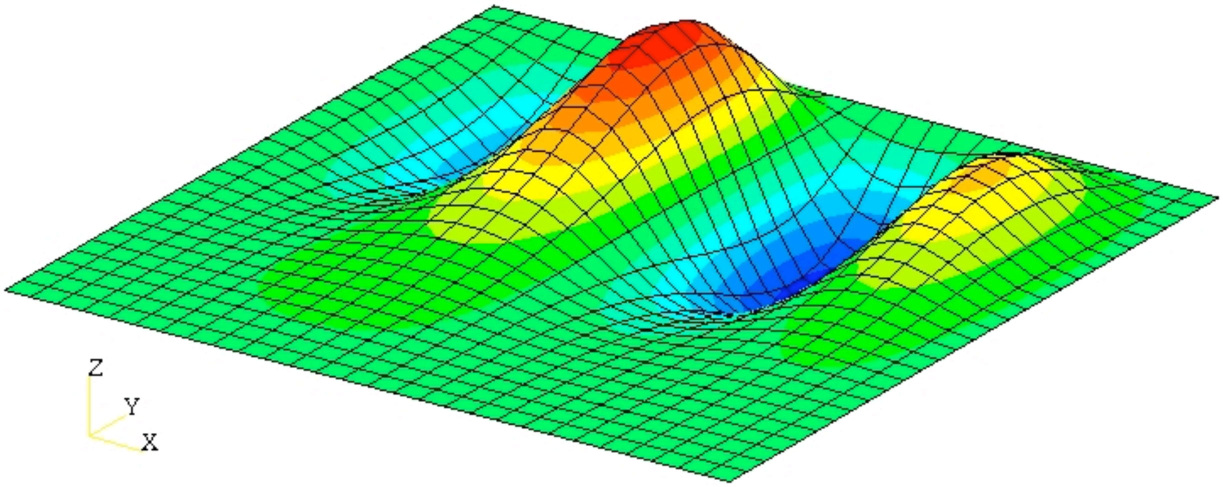

Figure 23: Fundamental mode shape for load case TB2_1

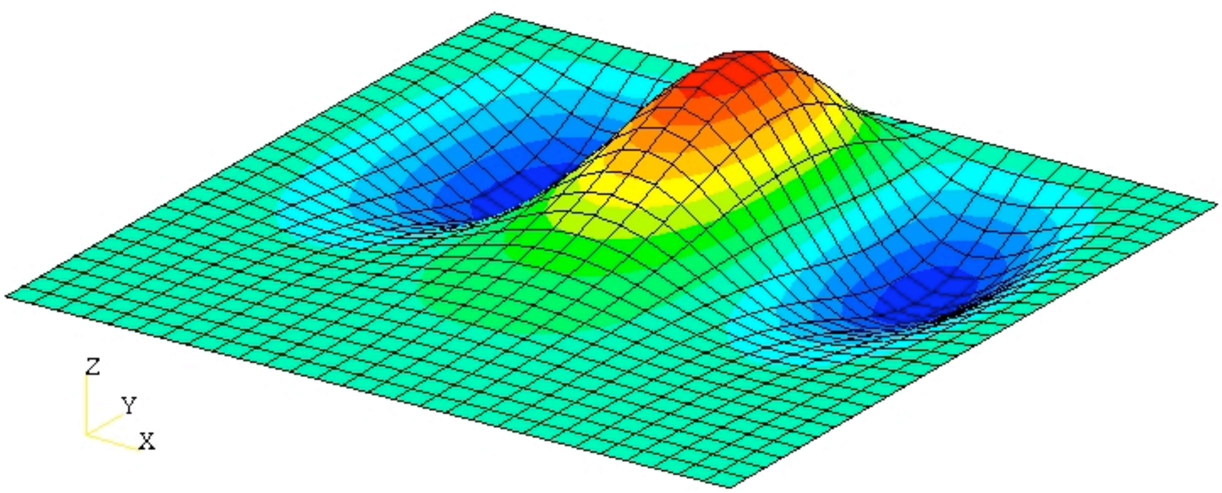

Figure 24: Fundamental mode shape for load case TB2_05

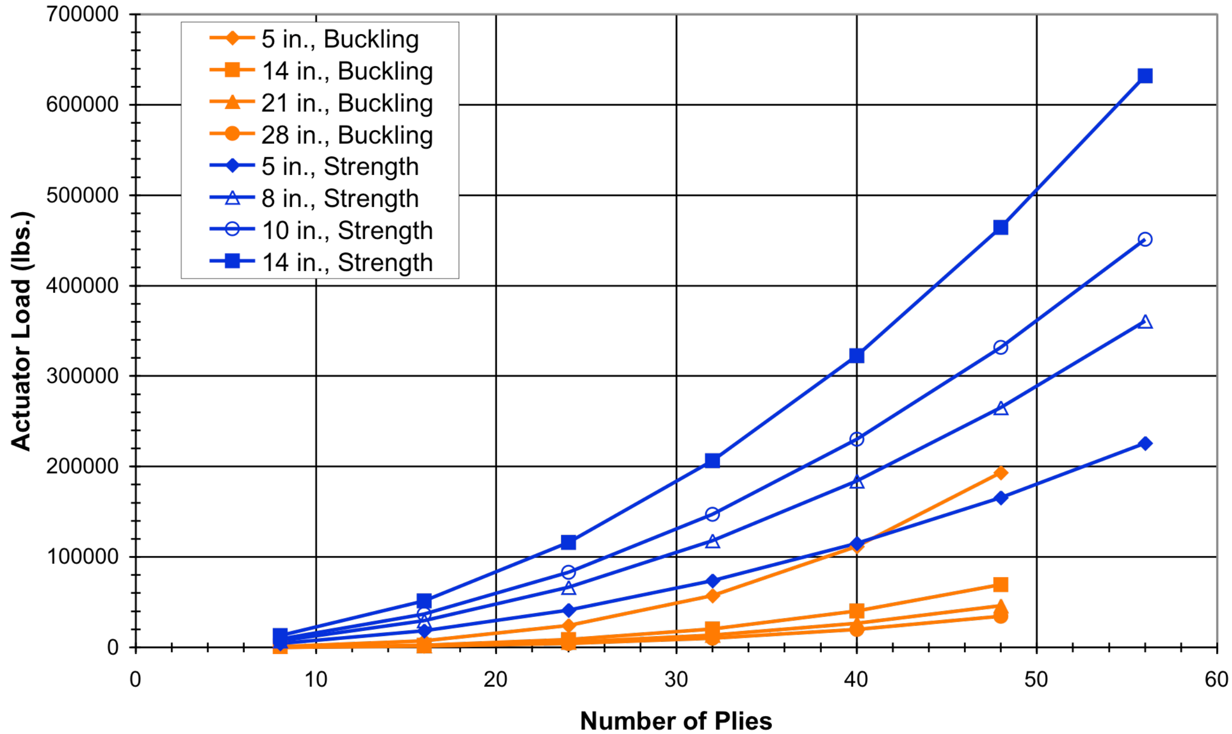

Figure 25: Tension actuator load, load case TC

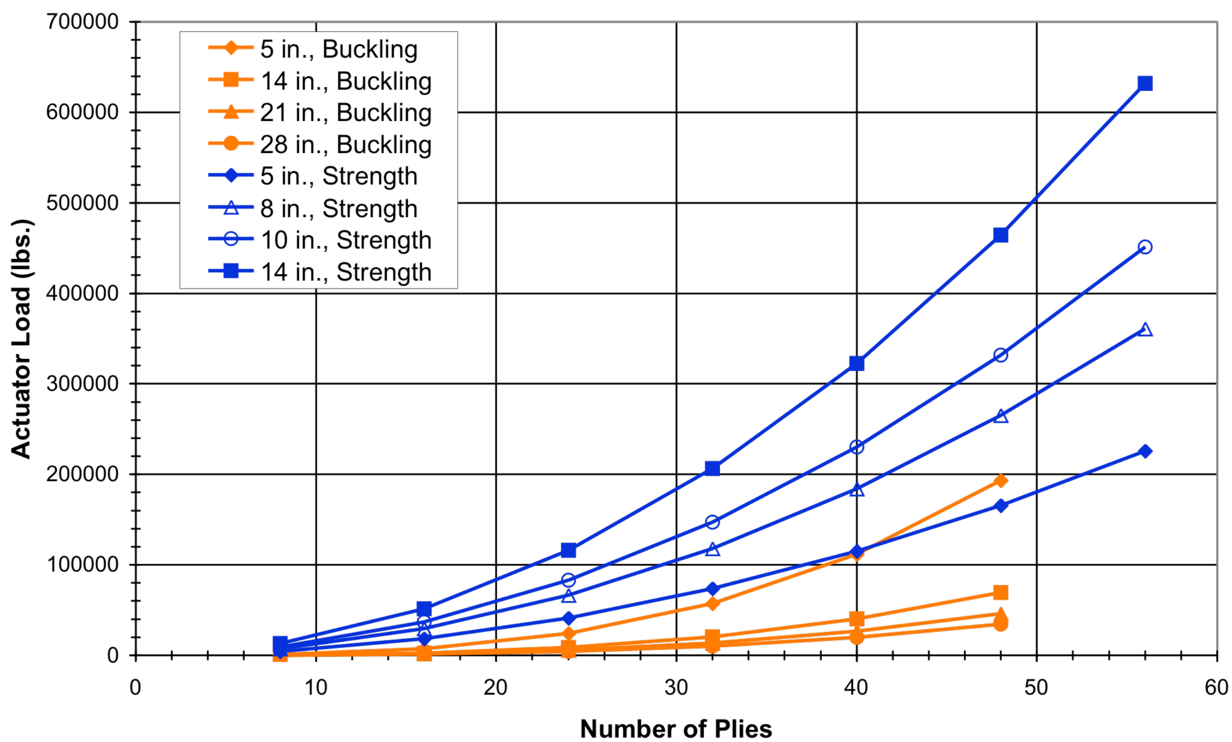

Figure 26: Compression actuator load, load case TC

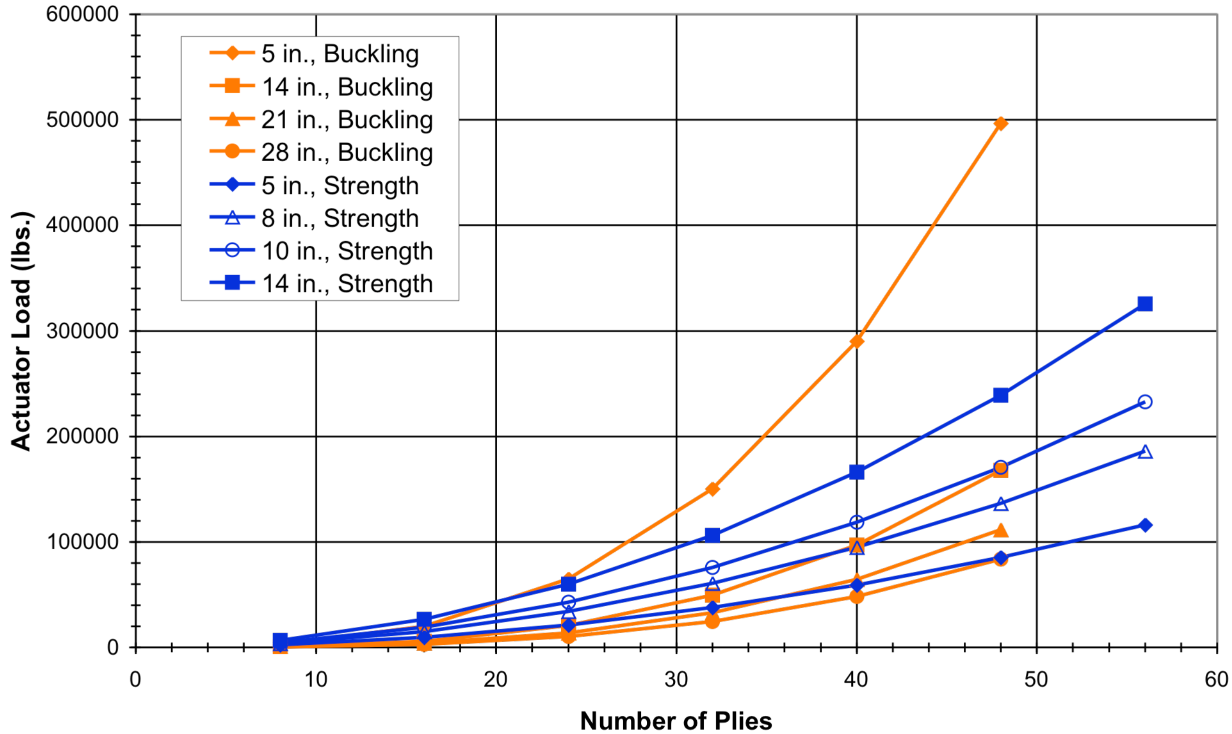

Figure 27: Tension actuator load, load case TS_1

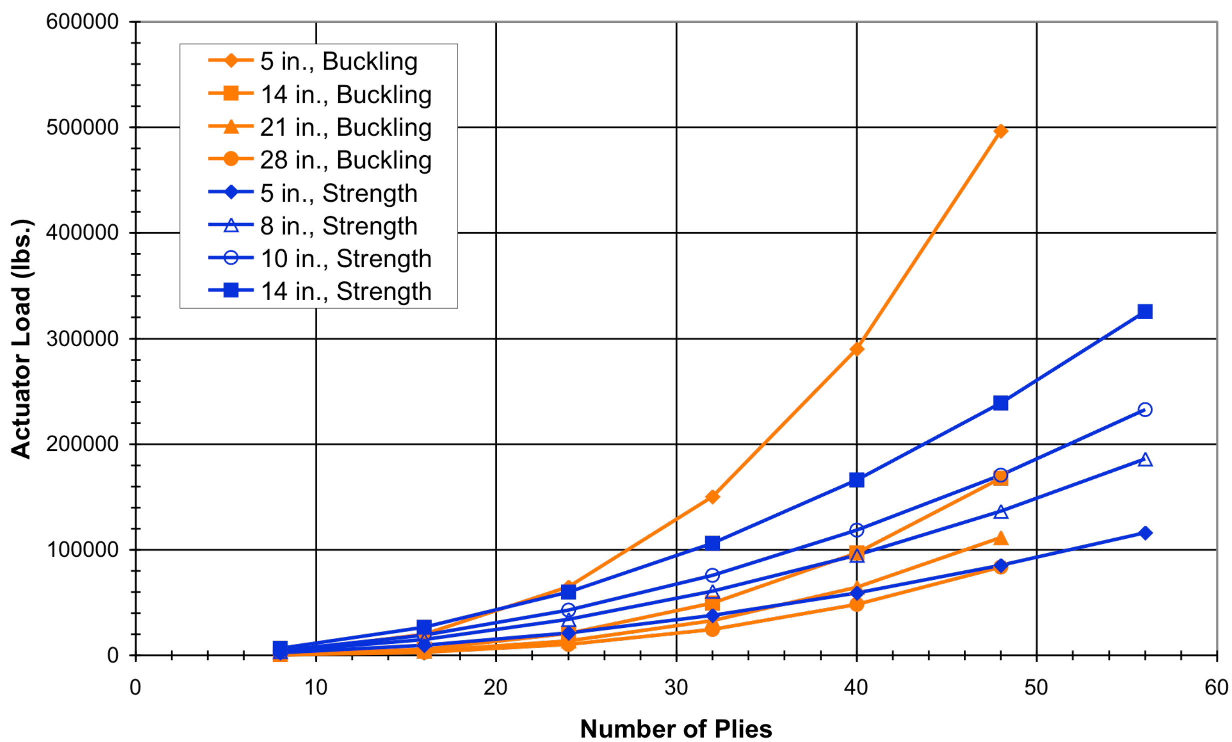

Figure 28: Shear actuator load, load case TS_1

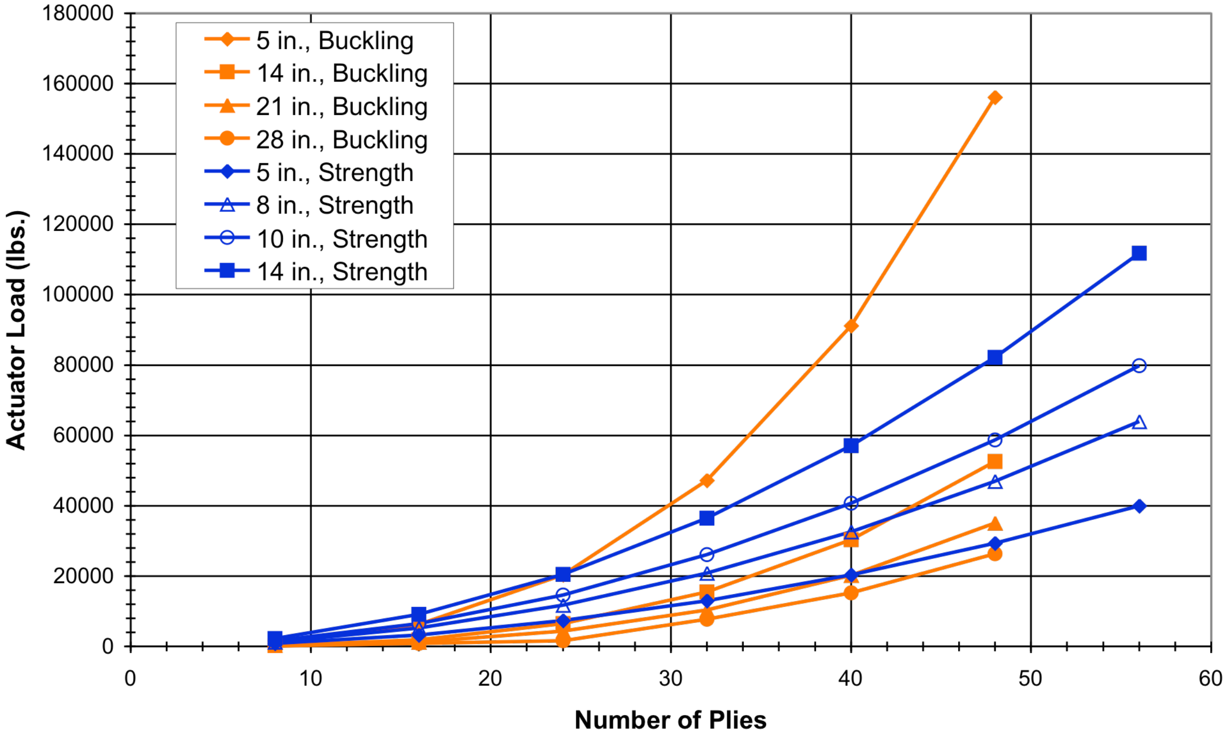

Figure 29: Tension actuator load, load case TS_05

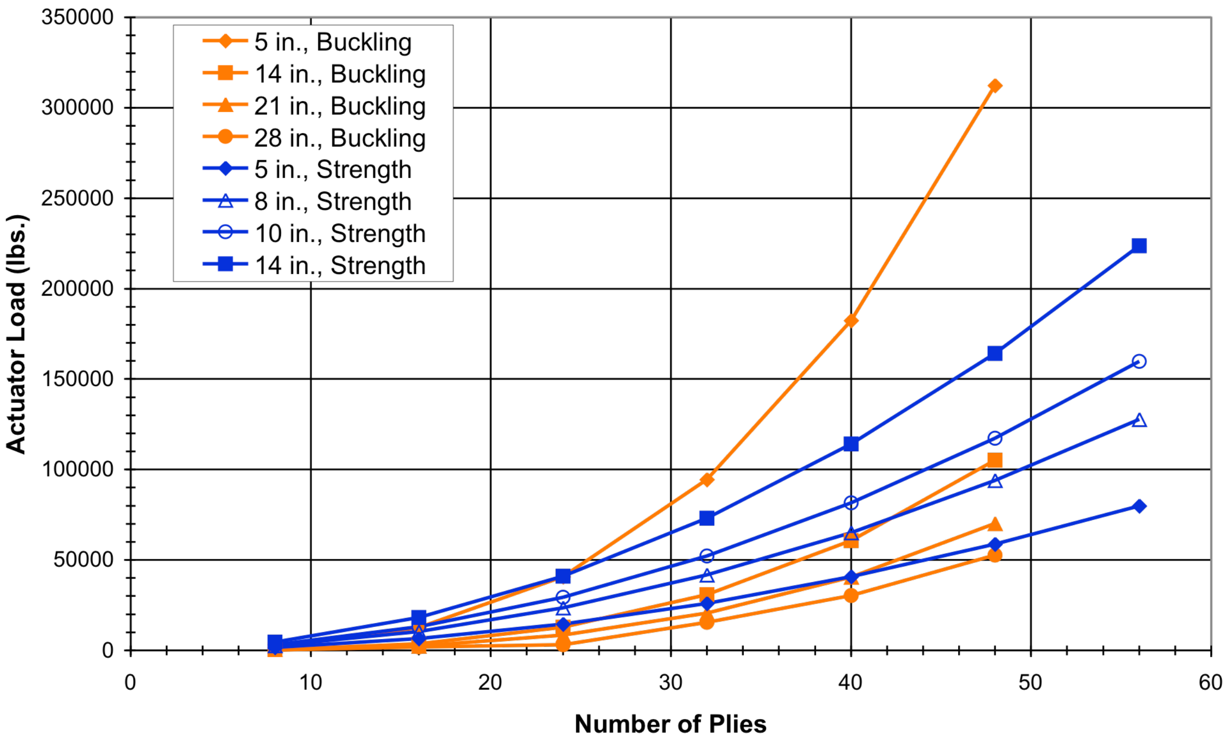

Figure 30: Shear actuator load, load case TS_05

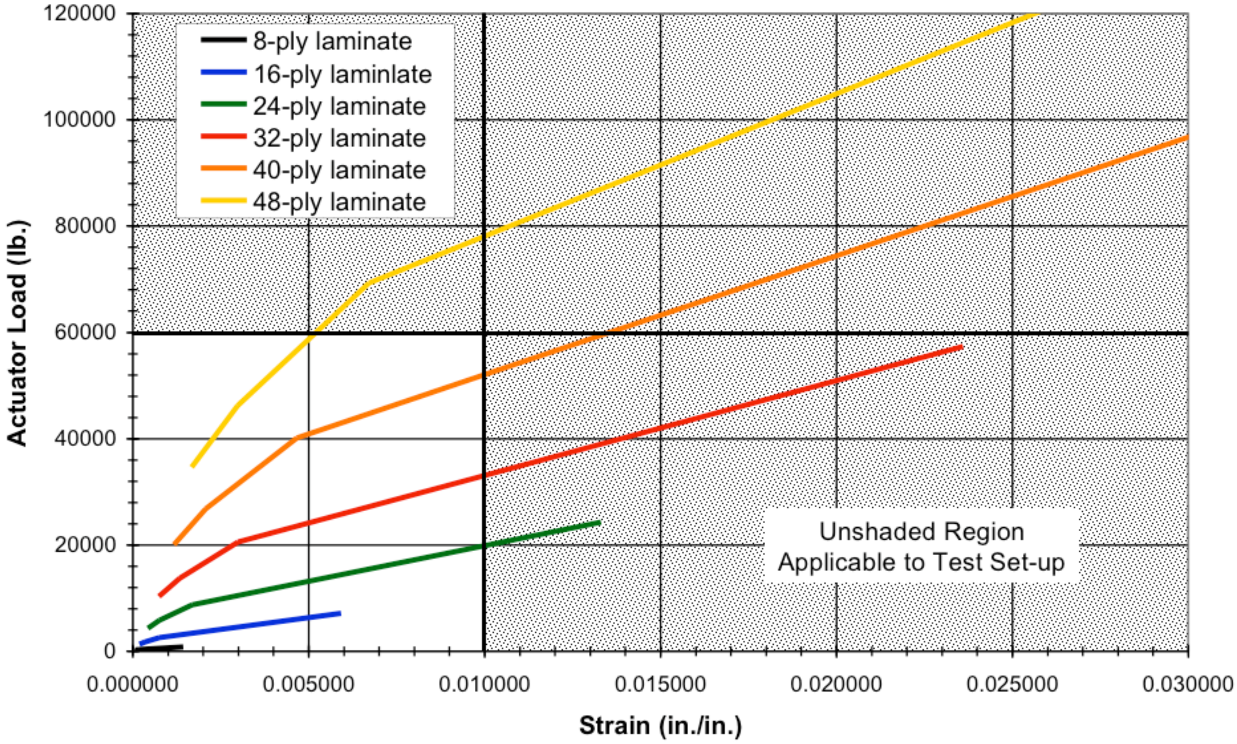

Figure 31: Tension actuator load/tension strain, load case TC, buckling

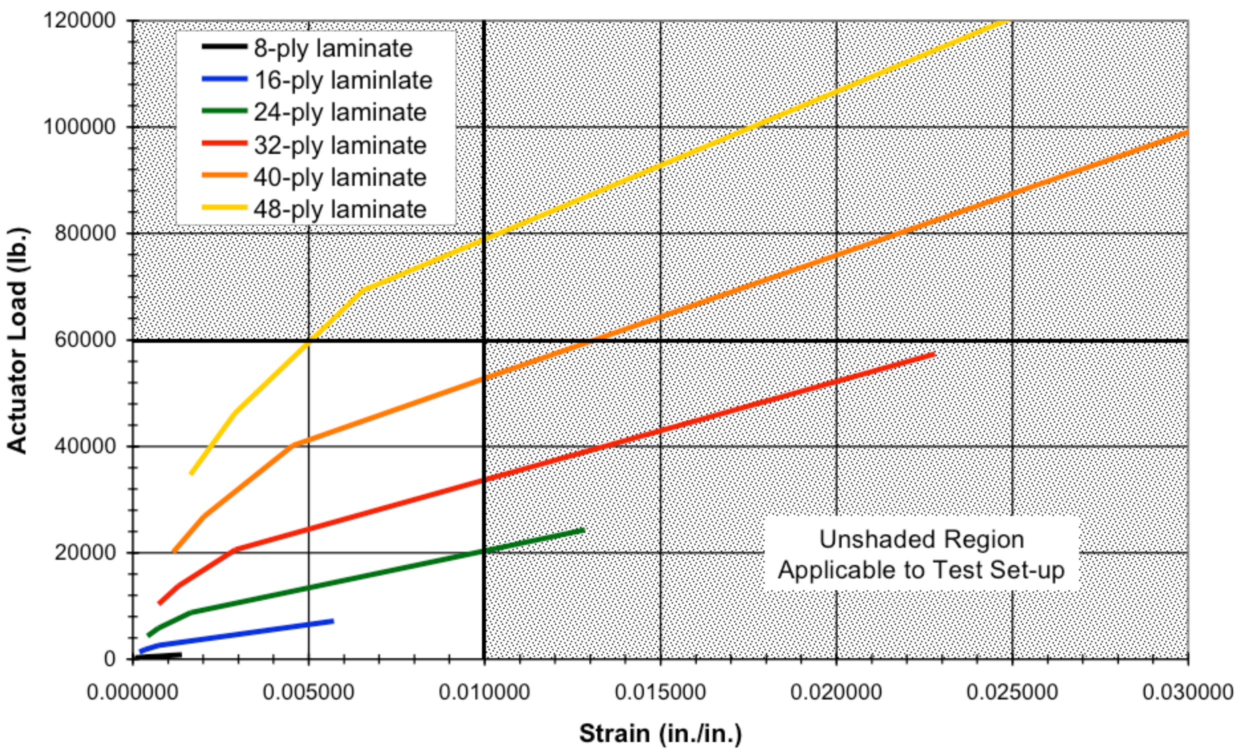

Figure 32: Compression actuator load/compression strain, load case TC, buckling

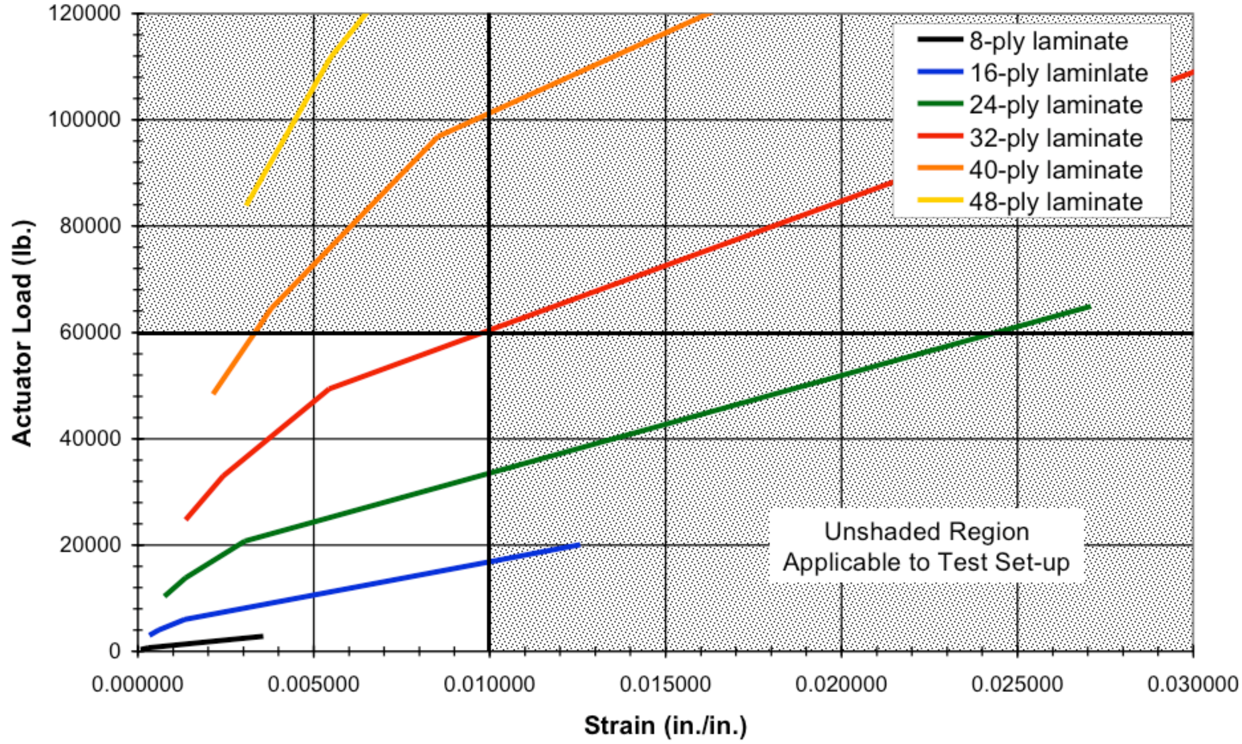

Figure 33: Tension actuator load/tension strain, load case TS_1, buckling

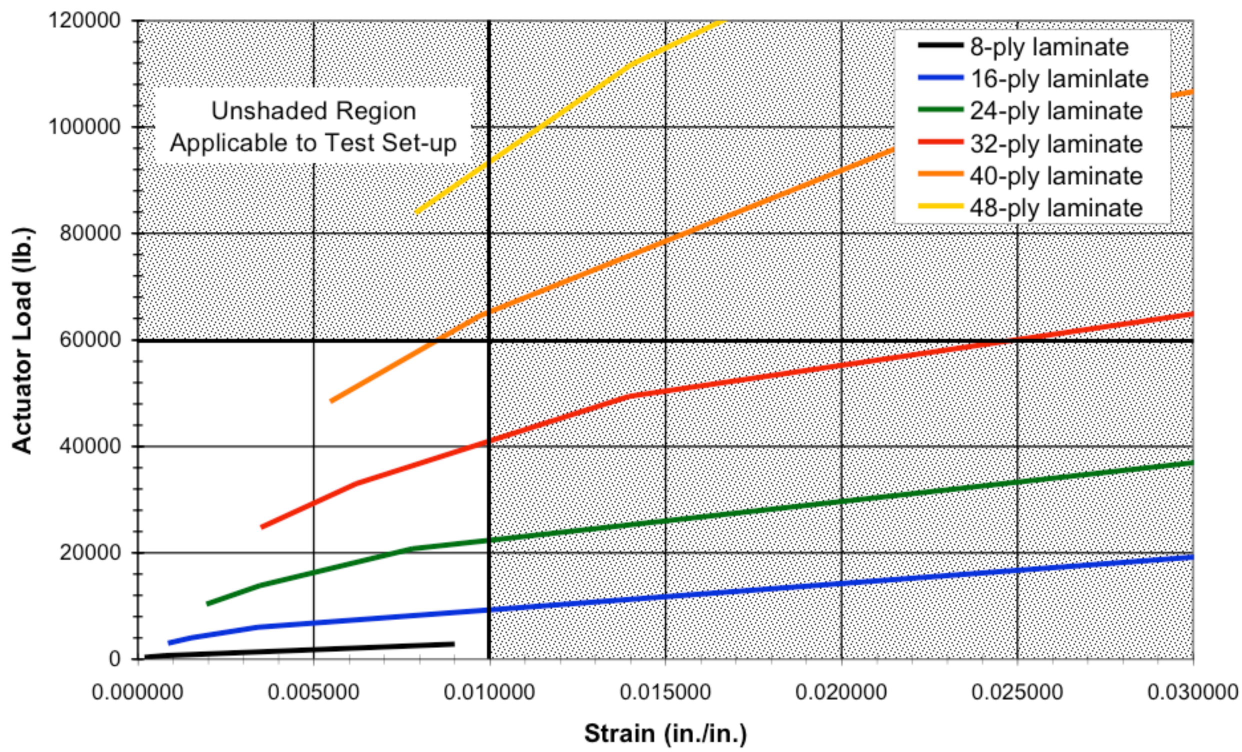

Figure 34: Shear actuator load/shear strain, load case TS_1, buckling

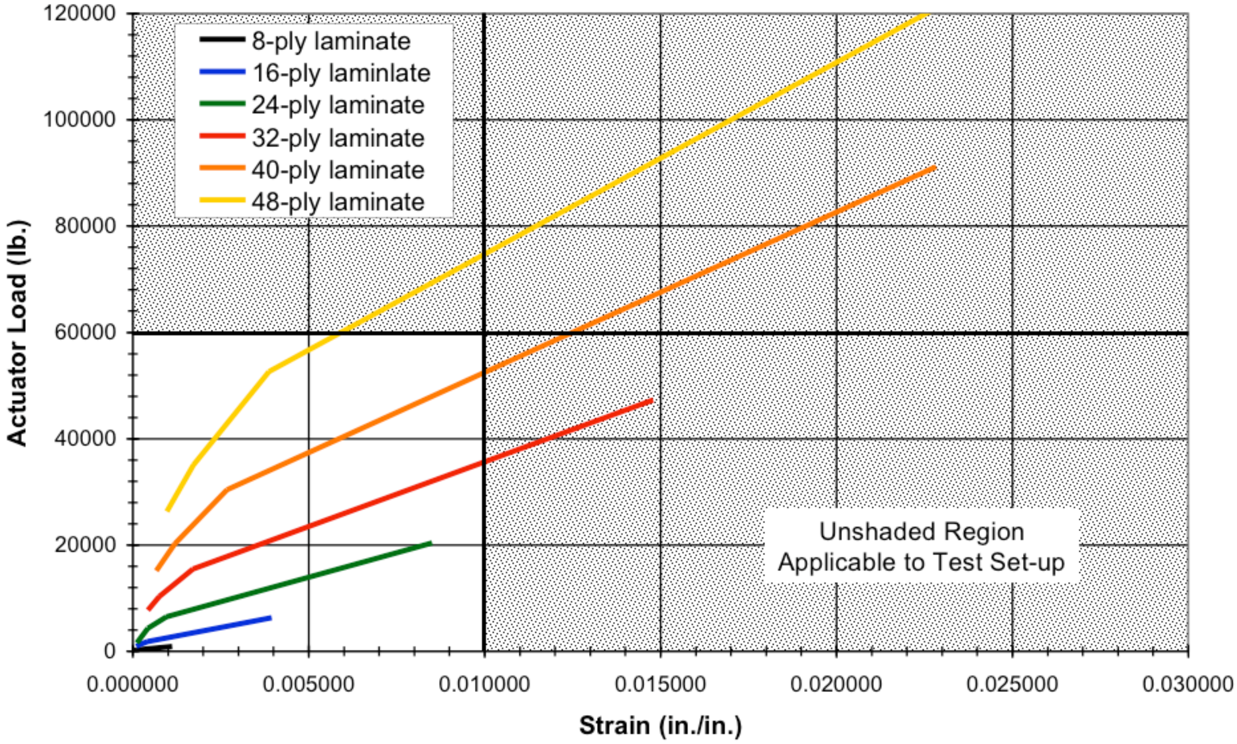

Figure 35: Tension actuator load/tension strain, load case TS_05, buckling

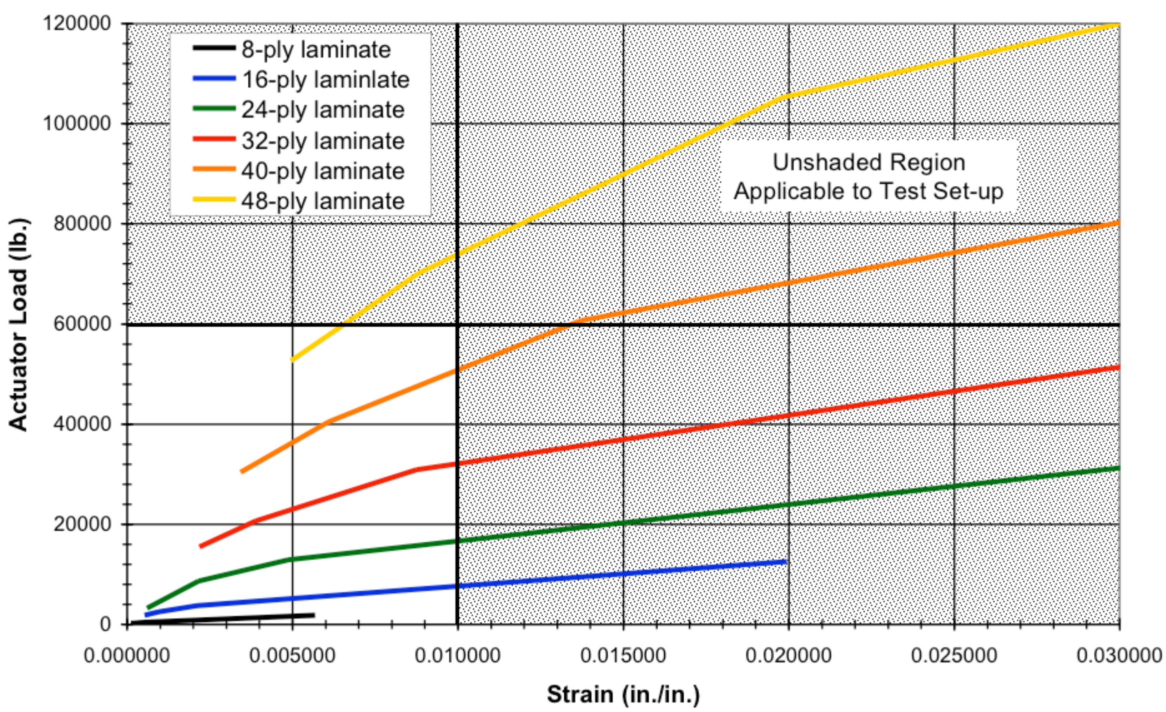

Figure 36: Shear actuator load/shear strain, load case TS_05, buckling

Summary/Conclusion

Several test configurations and constructions were analytically examined to determine their suitability for testing combined-loaded panels. Configurations included a D-box, segmented cylinder and single panel set-up. The current study indicates that the single panel configuration is the best choice for testing combined-loaded panels, particularly flat panels. The single-panel configuration is also capable of examining both strength- and buckling-critical test specimens, with specimens of much greater thickness than are possible the other configurations examined. However, due to its picture frame construction, the single panel configuration is not well suited for panels having curvature. Therefore, further study and design development is required to provide a test configuration better suited to curved panels under combined loads.

References

[1]Musgrove, Max D., and Green, Bruce E., "Advanced Beaded and Tubular Structural Panels", NASA-CR-2514, September 1975.

[2]Percy, W., "Buckling Analysis and Test Correlation of Hat Stiffened Panels for Hypersonic Vehicles", AIAA-1990-5219. AIAA Second International Aerospace Planes Conference, Orlando, FL, 29-31 October, 1990.

[3]Martin, Carl J., and McWithey, Robert R., "A Novel Concept for a Combined-Load Test Apparatus", AIAA-1991-1083. 32nd AIAA/ASME/ASCE/AHS/ASC Structures, Structural Dynamics and Materials Conference, Baltimore, MD, 8-10 April, 1991.

[4]Romeo, Giulio, and Frulla, Giacomo, "Postbuckling Behavior of Anisotropic Plates Under Biaxial Compression and Shear Loads", 18th Congress of the International Council of the Aeronautical Sciences, September 20-25, 1992, Beijing, People's Republic of China, pp. 1946-1944.

[5]Romeo, Giulio, and Frulla, Giacomo, "Nonlinear Analysis of Anisotropic Plates with Initial Imperfections and Various Boundary Conditions Subjected to Combined Biaxial Compression and Shear", *International Journal of Solids and Structures*, Vol. 31, No. 6, 1994, pp. 763-783.

[6]Romeo, Giulio, and Frulla, Giacomo, "Post-Buckling Behaviour of Graphite/Epoxy Stiffened Panels with Initial Imperfections Subjected to Eccentric Biaxial Compression Loading", *International Journal of Non-Linear Mechanics*, Vol. 32, No. 6, 1997, pp. 1017-1033.

[7]Romeo, Giulio, and Frulla, Giacomo, "Analytical/Experimental Behavior of Anisotropic Rectangular Panels Under Linearly Varying Combined Loads", *AIAA Journal*, Vol. 39, No. 5, May 2001, pp. 932-941.

[8]Romeo, Giulio, "Analytical and Experimental Behaviour of Laminated Panels with Rectangular Opening Under Biaxial Tension, Compression and Shear Loads", *Journal of Composite Materials*, Vol. 35 (2001), No. 8, pp. 639-663.

[9]Featherston, C. A., and Ruiz, C., "Buckling of Curved Panels Under Combined Shear and Compression", Journal of Mechanical Engineering Science, Part C, Vol. 212 (1998), No. 3, pp. 183-196.

[10]Featherston, C. A., and Ruiz, C., "Buckling of Flat Plates Under Bending and Shear", *Journal of Mechanical Engineering Science, Part C*, Vol. 212 (1998), No. 4, pp. 249-261.

[11]Ambur, Damodar R., Cerro, Jeffrey A., and Dickson, John, "D-Box Fixture for Testing Stiffened Panels in Compression and Pressure", *Journal of Aircraft*, Vol. 32, No. 6, November – December 1995, pp. 1382-1389.

[12]Rouse, Marshal, Young, Richard D., and Gehrki, Ralph E., "Structural Stability of a Stiffened Aluminum Fuselage Panel Subjected to Combined Mechanical and Internal Pressure Loads", AIAA-2003-1423. 44th AIAA/ASME/ASCE/AHS/ASC Structures, Structural Dynamics, and Materials Conference, Norfolk, VA, 7-10 April, 2003 .

[13]Fields, Roger A., Richards, W. Lance, and DeAngelis, Michael V., "Combined Loads Test Fixture for Thermal-Structural Testing Aerospace Vehicle Panel Concepts", NASA/TM-2004-212039.

[14]Wilkins, D. J., and Olson, F., "Shear Buckling of Advanced Composite Curved Panels", *Experimental Mechanics*, Vol. 14, 1974, pp. 326-330.
[15]Wolf, K., and Kossira, H., "An Efficient Test Method for the Experimental Investigation of the Postbuckling Behavior of Curved CFRP Laminated Shear Panels", Proceedings, ECCM-CTS, European Conference on Composite Testing and Standardisation, Amsterdam, September 8-10, 1992.
[16]*MSC.Patran Reference Manual*, MSC.Software Corporation, 2004.
[17]Rankin, Charles C., Brogan, Frank A., Loden, William A., and Cabiness, Harold D., *STAGS User Manual, Version 5.0*, Lockheed Martin Missiles & Space Co., Inc., Palo Alto, CA, March, 2003.

REPORT DOCUMENTATION PAGE

Form Approved
OMB No. 0704-0188

1. REPORT DATE *(DD-MM-YYYY)*	**2. REPORT TYPE**	**3. DATES COVERED** *(From - To)*
01- 10 - 2006	Contractor Report	

4. TITLE AND SUBTITLE
Configuration and Sizing of a Test Fixture for Panels Under Combined Loads

5a. CONTRACT NUMBER
NNL04AA10B

5b. GRANT NUMBER

5c. PROGRAM ELEMENT NUMBER

6. AUTHOR(S)
Lovejoy, Andrew E.

5d. PROJECT NUMBER

5e. TASK NUMBER

5f. WORK UNIT NUMBER
561581.02.08.07

7. PERFORMING ORGANIZATION NAME(S) AND ADDRESS(ES)
NASA Langley Research Center
Hampton, VA 23681-2199

Analytical Services & Materials, Inc.
107 Research Drive
Hampton, VA 23666-1340

8. PERFORMING ORGANIZATION REPORT NUMBER

9. SPONSORING/MONITORING AGENCY NAME(S) AND ADDRESS(ES)
National Aeronautics and Space Administration
Washington, DC 20546-0001

10. SPONSOR/MONITOR'S ACRONYM(S)
NASA

11. SPONSOR/MONITOR'S REPORT NUMBER(S)
NASA/CR-2006-214520

12. DISTRIBUTION/AVAILABILITY STATEMENT
Unclassified - Unlimited
Subject Category 39
Availability: NASA CASI (301) 621-0390

13. SUPPLEMENTARY NOTES
Langley Technical Monitor: Dawn C. Jegley
An electronic version can be found at http://ntrs.nasa.gov

14. ABSTRACT
Future air and space structures are expected to utilize composite panels that are subjected to combined mechanical loads, such as bi-axial compression/tension, shear and pressure. Therefore, the ability to accurately predict the buckling and strength failures of such panels is important. While computational analysis can provide tremendous insight into panel response, experimental results are necessary to verify predicted performances of these panels to judge the accuracy of computational methods. However, application of combined loads is an extremely difficult task due to the complex test fixtures and set-up required. Presented herein is a comparison of several test set-ups capable of testing panels under combined loads. Configurations compared include a D-box, a segmented cylinder and a single panel set-up. The study primarily focuses on the preliminary sizing of a single panel test configuration capable of testing flat panels under combined in-plane mechanical loads. This single panel set-up appears to be best suited to the testing of both strength critical and buckling critical panels. Required actuator loads and strokes are provided for various square, flat panels.

15. SUBJECT TERMS
Graphite-epoxy; Buckling; Testing

16. SECURITY CLASSIFICATION OF:			**17. LIMITATION OF ABSTRACT**	**18. NUMBER OF PAGES**	**19a. NAME OF RESPONSIBLE PERSON**
a. REPORT	**b. ABSTRACT**	**c. THIS PAGE**			STI Help Desk (email: help@sti.nasa.gov)
					19b. TELEPHONE NUMBER ***(Include area code)***
U	U	U	UU	53	(301) 621-0390